Psychological Review
1987, Vol. 94, No. 1, 84–106

560

Skilled Actions: A Task-Dynamic Approach

Elliot Saltzman

J. A. Scott Kelso

0033-295X/87/$00.75

Psychological Review
1987, Vol. 94, No. 1, 84–106

0033-295X/87/$00.75

Skilled Actions: A Task-Dynamic Approach

Elliot Saltzman
Haskins Laboratories, New Haven, Connecticut and
University of Connecticut

J. A. Scott Kelso
Florida Atlantic University and Haskins Laboratories,
New Haven, Connecticut

A task-dynamic approach to skilled movements of multi-degree-of-freedom effector systems is developed in which task-specific, relatively autonomous action units are specified within a functionally defined dynamical framework. Qualitative distinctions among tasks (e.g., the body maintaining a steady vertical posture or the hand reaching to a single spatial target versus cyclic vertical hopping or repetitive hand motion between two spatial targets) are captured by corresponding distinctions among dynamical topologies (e.g., point attractor versus limit cycle dynamics) defined at an abstract task space (or work space) level of description. The approach provides a unified account for several signature properties of skilled actions: trajectory shaping (e.g., hands move along approximately straight lines during unperturbed reaches) and immediate compensation (e.g., spontaneous adjustments occur over an entire effector system if a given part is disturbed en route to a goal). Both of these properties are viewed as implicit consequences of a task's underlying dynamics and, importantly, do not require explicit trajectory plans or replanning procedures. Two versions of task dynamics are derived (control law, network coupling) as possible methods of control and coordination in artificial (robotic, prosthetic) systems, and the network coupling version is explored as a biologically relevant control scheme.

For all animals to function effectively in their environments, their movements must be coordinated in space and time. How coordination and control arise in complex, multivariable systems and how the many musculoskeletal degrees of freedom are coordinated adaptively during skilled actions are fundamental issues currently under investigation in a number of disciplines (e.g., neuroscience, robotics, artificial intelligence, and cognitive science). Solutions to these problems may be hindered in part by a generic "limited ability to recognize the significant informational units of movement" (Greene, 1971, p. xviii; see also Szentagothai & Arbib, 1974). It is unlikely that these units are defined at the level of joints or muscles; rather, it can be argued on both empirical and theoretical grounds that musculoskeletal variables are partitioned into collective functional units of action (Bernstein, 1967; Whiting, 1984) or *coordinative structures* (e.g., Fowler, 1977; Kelso, Southard, & Goodman, 1979; Turvey, Shaw, & Mace, 1978). The behavior of these action units is often evidenced by invariant relationships among kinematic and muscular events during activities as diverse as postural control, locomotion, speech, handwriting, and reaching to a target (see Grillner, 1982; Kelso, 1981; Kelso, Tuller, & Harris, 1983; Nashner & McCollum, 1985; Schmidt, 1982; Viviani & Terzuolo, 1980).

The primary aim of the present article is to characterize the operation of these proposed coordinative structures in a so-called task-dynamic framework. By *task dynamics* we mean (a) that the degrees of freedom comprising action units are constrained by the particular tasks that animals perform and (b) that action units are specified in the language of dynamics rather than in terms of kinematic or muscular variables (cf. Stein, 1982). We describe an invariant control structure that is specified according to a task's dynamical requirements and that gives rise to diverse kinematic consequences. Although the task-dynamic framework is intended to apply equally to skilled actions of the limbs and speech articulators, the focus of the present article is on issues of control and coordination during a variety of sensorimotor tasks performed by the limbs. Preliminary applications of task dynamics to skilled movements of the speech articulators have been developed recently and are reported elsewhere (Kelso, Saltzman, & Tuller, 1986a, 1986b; Saltzman, 1986).

Our article is organized as follows: First we expand on those properties of action units that are central to the task-dynamic framework. Second, we present a short tutorial on topological dynamics in order to describe how a system's geometrical qualities are related to its dynamics in task-specific ways. Finally, we describe the task-dynamic approach and present two related versions (*control law* and *network coupling*). Task dynamics will

The preparation of this manuscript was supported in part by Contract No. N00014-83-C-0083 from the U.S. Office of Naval Research, National Institutes of Health Grant NS-13617, and Biomedical Research Support Grant RR-05596. Various aspects of the article have been formally presented at the Second International Conference on Event Perception, Nashville, Tennessee, June 1983, and at the Engineering Foundation Conference on Biomechanics and Neural Control, Henniker, New Hampshire, July 1983.

We would like to express our appreciation to the following colleagues for their helpful comments on an earlier draft and for valuable discussions concerning several of the topics therein: James Abbs, John Delatizky, Carol Fowler, Louis Goldstein, Vince Gracco, Neville Hogan, John Hollerbach, Fay Horak, Bruce Kay, Wynne Lee, Gin McCollum, Rich McGowan, Paul Milenkovic, Kevin Munhall, Lewis Nashner, Patrick Nye, Marc Raibert, and Michael Turvey. In addition, we are grateful to Phil Rubin, who developed some of the basic software procedures used in the present computer simulations.

Correspondence concerning this article should be addressed to Elliot Saltzman, Haskins Laboratories, 270 Crown St., New Haven, Connecticut 06511.

be shown to provide a viable account of tasks such as discrete reaching, bringing a cup to the mouth, and turning a handle. It can also offer a parsimonious account of various compensatory behaviors such as those that occur when an arm is perturbed during a reaching movement or when the support base is perturbed during standing. Finally, we suggest that the network coupling version of task dynamics both extends the control law version and synthesizes some recent physiological findings on the planning and control of arm trajectories.

The significance of task dynamics for theories of coordination and control is that it offers a unified account of certain phenomena that otherwise would require conceptually distinct treatments. In addition, the approach promises to be useful in the design and control of robotic and prosthetic devices. In fact, task dynamics shares some but not all of the features of several current developments in manipulator control (see Asada, 1982; Hogan & Cotter, 1982; Khatib, 1985; Koditschek, 1985; Raibert, Brown, Chepponis, Hastings, Shreve, & Wimberly, 1981; Takegaki & Arimoto, 1981). However, before discussing task dynamics in detail, we will describe the empirical phenomena—*trajectory shaping* and *immediate compensation*—that led us, in part, to develop the present theoretical approach.

The first phenomenon, trajectory shaping, refers to the task-specific motion patterns of the terminal devices or end effectors of the effector systems[1] used in various types of skills. For example, in reaching tasks involving two joints (shoulder and elbow) and two spatial dimensions of hand motion, it has been observed that the hands (a) move in quasi-straight-line spatial trajectories from initial to target positions and (b) display single-peaked tangential velocity curves (e.g., Morasso, 1981). Similarly and more obviously, in cup-to-mouth tasks the grasped cup maintains a spillage-preventing, approximately horizontal orientation en route from table to mouth.

The second phenomenon, immediate compensation, refers to the fact that skilled movements show task-specific flexibility in attaining the task goal. If one part of the system is perturbed, blocked, or damaged, the system is able to compensate (assuming the disturbance is not "too big") by reorganizing the activities of the remaining parts in order to achieve the original goal. Further, such readjustments appear to occur automatically without the need to detect the disturbance explicitly, replan a new movement, and execute the new movement plan. Kelso, Tuller, and Fowler (1982; see also Kelso, Tuller, Vatikiotis-Bateson, & Fowler, 1984; Munhall & Kelso, 1985) have demonstrated such behavior in the speech articulators (jaw, upper and lower lip, tongue body) when subjects produced the utterances /bæb/ or /bæz/ across a series of trials in which the jaw was occasionally and unpredictably tugged downward while moving upward to the final /b/ or /z/ closure (see also Abbs & Gracco, 1984; Folkins & Abbs, 1975). The system's response to the jaw perturbation was measured by observing the motions of the jaw and upper and lower lips as well as the electromyographic (EMG) activities of the orbicularis oris superior (upper lip), orbicularis oris inferior (lower lip), and genioglossus (tongue body) muscles. The investigators found relatively immediate task-specific compensation (i.e., 20–30 ms from onset of jaw pull to onset of compensatory response) in articulators remote to the jaw perturbation. For /bæb/ (in which final lip closure is crucial), they found increased upper lip activity (motion and EMG) relative to the unperturbed control trials but normal tongue activity; for /bæz/ (in which final tongue-palate constriction is important), they found increased tongue activity relative to controls but normal upper lip motion. The speed of these task-specific responses indicates that compensation occurs according to an automatic, reflexive type of organization. However, such an organization is not defined in a hard-wired input–output manner. Instead, these data imply the existence of a selective pattern of coupling or gating among the component articulators that is specific to the utterance produced. Essentially, then, such compensatory behavior represents the classic phenomenon of motor equivalence (Hebb, 1949; Lashley, 1930) whereby a system finds alternate routes to a given goal if its current route is unexpectedly blocked.

What type of sensorimotor organization could generate, in a task-specific way, both characteristic trajectory patterns for unperturbed movements and spontaneous, compensatory behaviors for perturbed movements? We believe that task dynamics provides at least the beginnings of a cohesive answer to this question. We start with an overview of action unit properties.

Units of Action

Action units display three major properties that are captured in a task-dynamic approach:

Functional Definition and Special Purpose Devices

Action units are defined abstractly in a functional, task-specific manner and span an ensemble of many muscles or joints. Thus, they are not defined in a traditional reductionist sense relative to single muscles and joints, nor are they hard-wired input–output reflex arrangements. These units serve to constrain their muscle/joint components to act cooperatively and specifically to the task at hand. For different skilled actions, performers transform the limbs temporarily into different *special purpose devices* whose functions match the tasks being performed. Thus, an arm can become a retriever, puncher, or polisher; a leg may become a walker or kicker; the body can become a dancer or swimmer; the speech organs may become talkers, singers, chewers, or swallowers, and so on.

Autonomy

Action units operate relatively autonomously and are, to a large extent, self-regulating. That is, once a given functional organization is established over a muscle/joint collective, the system achieves its goal with minimal voluntary intervention. In later discussions of the mathematics of task dynamics, we will also indicate that action units are relatively autonomous in a strict mathematical sense of time invariance; that is, the equations describing task-dynamic systems are not explicit functions of an independent time variable.

[1] An *effector system* is the set of limb segments or speech organs used in a given action; a *terminal device* or *end effector* is the part of an effector system that is directly related to the goal of a performed action. Thus, in a reaching task, the hand is the terminal device and the arm is the effector system; in a cup-to-mouth task, the grasped cup is the terminal device and the hand–arm system is the effector system; in a steady-state vowel production task, the tongue body surface is the terminal device and the jaw–tongue system is the effector system.

Dynamics

Action units are defined in the language of dynamics, not kinematics (e.g., Fowler, Rubin, Remez, & Turvey, 1980; Kelso, Holt, Kugler, & Turvey, 1980; Kugler, Kelso, & Turvey, 1980). The behaviors of an effector system are governed by task-specific control regimes. Such control regimes are defined by task-specific relationships among the system's dynamic parameters (e.g., stiffness, damping), and these relationships are specified according to the abstract functional demands of the performed skill. These control regimes serve to convert an effector system into the appropriate task-demanded special purpose device. Furthermore, a given dynamical regime generates motions that are characteristic of a particular skill and underlies the system's ability to compensate spontaneously for unpredicted disturbances. There is no explicit plan for the desired kinematic trajectory in the action unit, nor is there an explicit contingency table of replanning procedures for dealing with unexpected perturbations. Instead, task-specific kinematic trajectories and compensatory behaviors emerge from, or are implicit consequences of, the action unit's dynamics. In this sense, most robots (with at least one notable exception, i.e., Raibert et al., 1981) have no skills but are general-purpose devices that use the same dynamical control regime for all types of tasks, for example, spatial trajectory planning for the terminal device, conversion to a joint velocity plan, and joint velocity servoing for both manipulators (e.g., Whitney, 1972) and hexapod walker legs (e.g., McGhee & Iswandhi, 1979).

Given the above three points, we formulate the problem of skill learning as that of designing an action unit or coordinative structure whose underlying dynamics are appropriate to the skill being learned. That is, in acquiring a skill one is establishing a one-to-one correspondence between the functional characteristics of the skill and the dynamical regime underlying the performance of that skill. The issue of skill learning per se is beyond the scope of the present article. However, the correspondence between dynamics and function is perhaps the key concept underlying the task-dynamic approach. To explore it more fully we will (a) examine the geometric notion of topology as it relates to a system's dynamics and (b) describe how functionally specific dynamical topologies can be used to specify task-specific action units or coordinative structures.

Topology and Dynamics

Quite (and perhaps too) simply in the context of skilled action, topology refers to the qualitative aspects of a system's dynamics. By *qualitative* we mean, for example, whether a system's dynamics generate either a discrete motion to a single target or a sustained cyclic motion between two targets. For a one-degree-of-freedom rotational system such as the elbow joint (flexion–extension degree of freedom), a positioning task to a given joint angle target would exemplify the first motion type. A reciprocal tapping task between two joint angle targets would exemplify the second motion type. What sort of dynamics might underlie these qualitatively different tasks? For the discrete task, several investigators have hypothesized that the system can be modeled as a damped mass-spring system (e.g., Cooke, 1980; Fel'dman, 1966; Kelso, 1977; Kelso & Holt, 1980; Polit & Bizzi, 1978; Schmidt & McGown, 1980). Such a dynamical system is described by the following equation of motion:

$$I\ddot{x} + b\dot{x} + k(x - x_0) = 0, \quad (1)$$

where I = moment of inertia about the rotation axis;
b = damping (friction) coefficient;
k = stiffness coefficient;
x_0 = equilibrium angle; and
$x, \dot{x}, \ddot{x}$ = angular displacement and its respective first and second time derivatives.

If we assume a set of constant dynamic parameters (I, b, k, x_0), then the behavior of this autonomous (time-invariant) system can be characterized by its *point stability* or *equifinality.* That is, it will come to rest at the specified x_0 target from various initial conditions for x and $\dot{x}$ and despite any transient perturbations encountered en route to the target.

The behavior of such systems can be displayed graphically in two different ways. In Figure 1A, the angle of an underdamped mass-spring with constant coefficients is plotted as a function of time for a given set of initial conditions and with no perturbations introduced. Defining the equilibrium or rest angle as aligned with the abscissa, the system's point stability is evidenced by the progressive decay of the motion to the steady-state rest angle. In Figure 1B, the same behavior is represented in the phase plane where the abscissa and ordinate correspond to x and $\dot{x}$, respectively, and the system's x_0 is located at the origin. In the phase plane, the system's point stability is evident in the motion's spiraling decay to the origin. Theoretically, if one were to plot the phase plane trajectories corresponding to all possible initial conditions, one would fill the plane with qualitatively similar decaying trajectories. This family of trajectories would define the system's *phase portrait.* The qualitative form of the system's phase portrait reflects the system's underlying dynamical topology, that is, the set of characteristic relations among the system's dynamic parameters. For the type of system described by Equation 1, the corresponding phase portrait represents the topology of a *point attractor* (Abraham & Shaw, 1982), and the underlying dynamics may be described as point attractor dynamics. As a model for positioning tasks, point attractor dynamics are appealing because the same underlying topology can generate discrete motions to a variety of targets with varying trajectory characteristics (e.g., peak velocity, movement time). These target and trajectory details are related to the specific values of the system's dynamic parameters.

Obviously, however, a different type of dynamics is required to generate a sustained cyclic elbow rotation (or finger rotation, e.g., Kelso, Holt, Rubin, & Kugler, 1981) between two target angles. Perhaps the simplest dynamical candidate is that of a time-invariant, undamped mass-spring system or harmonic oscillator. Its equation of motion is

$$I\ddot{x} + k(x - x_0) = 0 \quad (2)$$

(all symbols are as defined as in Equation 1). The solid line trajectory in Figure 2A represents the phase plane orbit of such a system, which oscillates about the origin (x_0) with an amplitude that is determined by the system's total mechanical energy and whose angular targets correspond to the system's maximum and minimum angular limits. However, this type of system is not a satisfactory model for cyclic elbow tasks for two reasons. First, it represents the ideal frictionless case, and no real-world system

is frictionless. Adding linear friction to Equation 2 simply converts it to Equation 1, leaving point attractor dynamics that are unsuitable for sustained cyclic tasks. Second, the system described by Equation 2 is only neutrally stable in that the oscillation is sensitive to both initial system energy (determined by initial conditions of position and velocity) and transient changes (perturbations) in energy imposed during motion. For example, both the solid and dotted trajectories in Figure 2A represent oscillations of the same system. However, the inner and outer dotted orbits correspond to smaller and larger amplitude initial conditions, respectively, relative to the solid orbit. For an oscillatory task whose amplitude is crucial, a neutrally stable system is clearly undesirable.

The shortcomings of neutral stability for cyclic tasks can be overcome by moving to a time-invariant *periodic attractor* (Abraham & Shaw, 1982) dynamical regime, with the following equation of motion:

$$I\ddot{x} + b\dot{x} + k(x - x_0) = f(x, \dot{x}), \tag{3}$$

where $I, b, k, x_0, x, \dot{x}, \ddot{x}$ are as in Equations 1 and 2; and

$f(x, \dot{x})$ = nonlinear escapement function of the system's current $x, \dot{x}$.

This system's behavior is exemplified in Figure 2B by three phase plane trajectories that correspond to different sets of initial conditions. The solid trajectory represents a motion starting at either target, and the inner and outer dotted trajectories represent motions starting inside and outside, respectively, of the target-to-target angular range. These latter trajectories converge onto the solid orbit, which is described as the system's stable *limit cycle* or periodic attractor. In fact, all trajectories (except those starting exactly at x_0) converge to the limit cycle, and the corresponding phase portrait captures this periodic attractor topology. The reason for this *orbital stability* lies in the nature of the nonlinear *escapement* term, $f(x, \dot{x})$, seen in Equation 3.[2] The escapement allows the system to tap an external energy source in a self-gated way; that is, energy is gated into or out of the system as a function of the system's current $x, \dot{x}$ state. On the limit cycle, the energy tapped per cycle from the external source is equal to the energy dissipated per cycle by both the system's intrinsic damping properties (i.e., $b\dot{x}$) and the system's escapement. Inside the limit cycle, the energy tapped per cycle is greater than that dissipated, and trajectories grow or spiral out to the limit cycle; outside the limit cycle, the converse is true and trajectories decay or spiral down to the limit cycle (see Minorsky, 1962).

The above examples show how distinct tasks (discrete positioning vs. cyclic alternation) may be modeled by topologically distinct dynamical systems. However, in these examples both

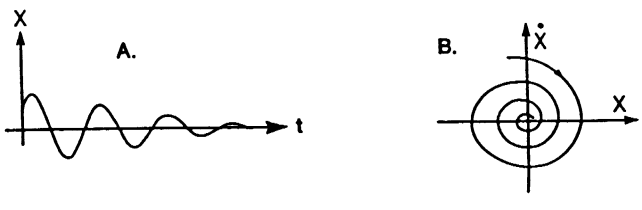

Figure 1. Point attractor system (A: position versus time; B: velocity versus position [phase portrait]).

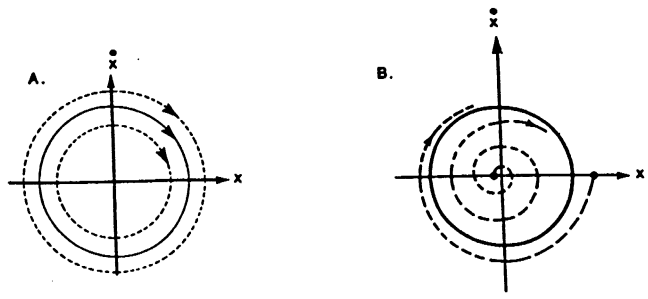

Figure 2. Phase portraits for neutrally stable system (A) and periodic attractor system (B), showing system trajectories for several initial conditions.

tasks and dynamics were defined by single degrees of freedom. One-dimensional motions were demanded by the tasks, and these task requirements mapped directly onto time-invariant, dynamical regimes for a single joint. We call this style of control *articulator dynamics*, because it involves defining task-specific sets of constant dynamic parameters for the control of motions at single joints or articulatory degrees of freedom. Real-world tasks seldom involve such simple one-to-one mappings between task demands and dynamical regimes. Consider, for example, the two-dimensional reaching task described earlier in this article. This task involved two articulatory degrees of freedom (shoulder, elbow) and two spatial dimensions of terminal device (hand) motion. Extending an articulator-dynamics approach to this more complex task is only partially successful. It provides a reasonable account of final position control but fails to account for the quasi-straight-line trajectory patterns of the hand (Delatizky, 1982). More specifically, in this two-dimensional task there is a unique mapping from hand position to arm configuration (i.e., the set of shoulder and elbow angles, arm posture) due to both the nonredundancy[3] of the arm (e.g., Saltzman, 1979) and the anatomical limits of joint angular excursion. Therefore, constant point attractor dynamics can be defined at each joint, with rest angles corresponding to the target arm configuration (and thus target hand position). In such cases, the hand/arm will show equifinality and attain the target position/configuration despite variations in initial position/

[2] Different limit cycle systems may have different types of escapements (e.g., Jordan & Smith, 1977). For example, van der Pol and Rayleigh oscillators have related escapement terms that are continuous functions of the systems' states; the pendulum clock's escapement term is a discontinuous function of the system's state, injecting a pulse of energy at one or two discrete points in the cycle.

[3] For a task in which an arm is nonredundant, the number of controlled spatial variables for the terminal device is equal to the number of controlled joint angular variables for the arm. Hence, the inverse kinematic transformation from spatial motions of the terminal device to corresponding arm joint angular motions is determinate. For a task in which the number of joint variables exceeds the number of spatial variables, this transformation is indeterminate and the arm is redundant. For redundant arms, one may specify the inverse kinematic transformation by (a) "freezing" the extra joints in the arm, (b) adding extra controlled spatial variables to the task description, or (c) specifying optimality criteria to be satisfied for the joint variables during the movement.

posture and despite transient disturbances encountered en route to the target. However, as mentioned above (and to be explained in greater detail below), this articulator-dynamics approach fails to account for the trajectory patterns seen in these reaching tasks and does not "favor straight line movements over other movements" (Hollerbach, 1982, p. 190).

The elegance of the articulator-dynamic account for single-degree-of-freedom tasks lies in its use of task-specific and time-invariant dynamical regimes to generate a potentially infinite number of task-appropriate kinematic trajectories. The failure of such an approach when extended to trajectory shaping in a multi-degree-of-freedom reaching task shows that invariant, task-specific action units are probably not defined at the level of articulatory degrees of freedom. What type of principles or control structures might underlie the trajectory constraints on arm motion during reaching tasks? There are (at least) two alternative accounts. The first is simply to abandon a dynamical approach altogether and to invoke explicit kinematic trajectory plans as sources for the characteristic constraints on motion patterns observed in different tasks. Such an approach has been generally adopted in the field of robotics (e.g., Hollerbach, 1982; Saltzman, 1979) and has been described in the following fashion by Hollerbach (1982):

> A hierarchal movement plan is developed at three levels of abstraction. . . . The top level is the object level, where a task command, such as 'pick up the cup,' is converted into a *planned trajectory* [italics added] for the hand or for the object held by the hand. At the joint level the object trajectory is converted to co-ordinated control of the multiple joints of the human or robotic arm. At the actuator level the joint movements are converted to appropriate motor or muscle activations. (p. 189)

Alternatively, a second account involves defining control regimes at a level of task description that is more abstract than the level of individual joints or articulatory degrees of freedom.[4] This latter approach led us to a task-dynamic account of skilled actions.

Task Dynamics

All multivariable, real-world tasks share two characteristics: (a) they are typically defined for the terminal devices associated with task-relevant, multi-degree-of-freedom effector systems (e.g., the grasped cup and arm–trunk, respectively, for a cup-to-mouth task), and (b) they typically demand characteristic patterns of motion or force[5] by these terminal devices relative to a set of task-specific spatial axes or degrees of freedom. Thus, a given task type can be associated with a corresponding task-spatial coordinate system (*task space*) that is defined relative to both the terminal devices and the environmental objects or surfaces that are relevant to the task's performance. In fact, on the basis of evidence from a pointing task involving the elbow joint, Soechting (1982) has argued that the controlled variable for this task is not joint angle per se. Instead it appears to be the orientation angle of the forearm in a spatial coordinate system referenced to the environment (e.g., the floor surface, or gravity vector, etc.) or the actor's trunk. This view is consistent with the notion that a task-spatial coordinate system might indeed be the appropriate level at which to characterize skilled actions.

The central tenet of the task-dynamic approach is that an autonomous (time-invariant) dynamical system can be defined for each dimension of a given skill's task space. This process establishes a one-to-one correspondence between the functional characteristics of the skill and the task-dynamical topology underlying that skill's performance. In other words, skill-invariant action units are defined in a functional way, relative to a given skill's task space and corresponding task-space dynamics (more simply, task dynamics). These time-invariant task dynamics are used to define articulator-level dynamic parameters (e.g., joint stiffnesses, dampings, rest angles, etc.) that change during movement according to two related versions (*control law* and *network coupling*) of the task-dynamic model. These evolving task-specific constraints on articulator dynamics convert a given skill's effector system into an appropriate special purpose device whose individual components (i.e., articulatory degrees of freedom) act cooperatively in a manner specific to the task at hand. It should be remembered for purposes of comparison that the articulator-dynamics approach postulated time-invariant dynamical systems at the individual joint level. In contrast, the task-dynamic approach postulates time-invariant dynamical regimes at the task-space level for given types of multivariable tasks. A given set of task-space regimes would (a) underlie directly the changing patterns of "lower level" articulator-dynamic parameters and (b) ultimately underlie the task-specific trajectory patterns and compensatory behaviors observed during task performances. We now provide an overview of the specifics of the task-dynamic approach and use a relatively simple arm-reaching task for illustrative purposes. A schematic of the approach and the coordinate transformations involved is shown in Figure 3.

Task Dynamics and Task Network

Task space. Task-dynamic modeling for a given skill begins with an abstract, functional description of that skill's task

---

[4] Indeed, herein lies an important difference between the various versions of the mass-spring model (or equilibrium point hypothesis) for discrete targeting behavior. In one widespread view that is restricted to single-degree-of-freedom motions, muscles are represented by a pair of springs acting across a hinge in the agonist–antagonist configuration. The final equilibrium point is established by selecting a set of length–tension properties in opposing muscles (e.g., Bizzi, 1980; Cooke, 1980; Kelso, 1977). This view, at best, may work for deafferented muscle, but as pointed out by Fel'dman and Latash (1982, p. 178), it is inadequate for muscles in natural conditions. Moreover, as we discuss in the text, it does not work for complex, multivariable tasks. An alternative and more viable view is that the parallel between a single muscle and a spring is not a literal one. Instead, the mass-spring model is better viewed as a model of equifinality or motor equivalence: It is this abstract functional property that particular behaviors share with a mass-spring system (Kelso et al., 1980; Kelso & Saltzman, 1982). In short, the former articulator-dynamic version is a hypothesis about a physiological mechanism whose shortcomings have been noted (Bizzi, Accornero, Chapple, & Hogan, 1982; Fel'dman & Latash, 1982). The latter abstract dynamic version is a hypothesis about the functional properties of a complex behavioral system.

[5] Currently, our task-dynamic formulation does not include precision force control tasks. It can be easily adapted for tasks that demand particular motion patterns along a surface and only approximate control of the force exerted by the terminal device normal to the surface (e.g., polishing a car, erasing a blackboard). The approach can also be adapted for precision force control tasks, however, as demonstrated by Hogan and Cotter (1982).

space. Such a description has three parts. First, the relevant terminal devices and goal objects or surfaces are defined. Second, an appropriate number of task axes or degrees of freedom are defined relative to the terminal device and goal referents, and finally, an appropriate type of task-dynamic topology is defined along each task axis.[6] For a discrete reaching task in two spatial dimensions, the corresponding task space is modeled as a two-dimensional point attractor and is illustrated in Figure 4A. In this figure, the reach target (x) defines the origin of a t_1t_2 Cartesian coordinate system. Axis t_1 (the "reach axis") is oriented along the line from the target to the initial position of the terminal device (open circle), which is modeled as an abstract point *task mass*. Axis t_2 is defined orthogonal to t_1 and measures deviations of the task mass from the reach axis. The task mass is allowed to assume any t_1t_2 position (filled circle) during task performance and may be considered an abstract point mass because it is not tied to any particular effector system. The equations of motion corresponding to axes t_1 and t_2 are as follows:

$$m_T\ddot{t}_1 + b_{T_1}\dot{t}_1 + k_{T_1}t_1 = 0, \qquad (4)$$
$$m_T\ddot{t}_2 + b_{T_2}\dot{t}_2 + k_{T_2}t_2 = 0;$$

where m_T = task-mass coefficient;
b_{T_1}, b_{T_2} = damping coefficients; and
k_{T_1}, k_{T_2} = stiffness coefficients.

In Figure 4A the corresponding damping and stiffness elements are represented in lumped form by the squiggles in the lines connecting the task mass to axes t_1 and t_2. Equation 4 describes a linear, uncoupled set of task-space equations, whose terms are defined in units of force and whose dynamic parameters are constant. This equation can be represented in matrix form:

$$M_T\ddot{\mathbf{t}} + B_T\dot{\mathbf{t}} + K_T\mathbf{t} = \mathbf{0}, \qquad (5)$$

where

$$M_T = \begin{bmatrix} m_T & 0 \\ 0 & m_T \end{bmatrix}; \; B_T = \begin{bmatrix} b_{T_1} & 0 \\ 0 & b_{T_2} \end{bmatrix}; \; K_T = \begin{bmatrix} k_{T_1} & 0 \\ 0 & k_{T_2} \end{bmatrix}.$$

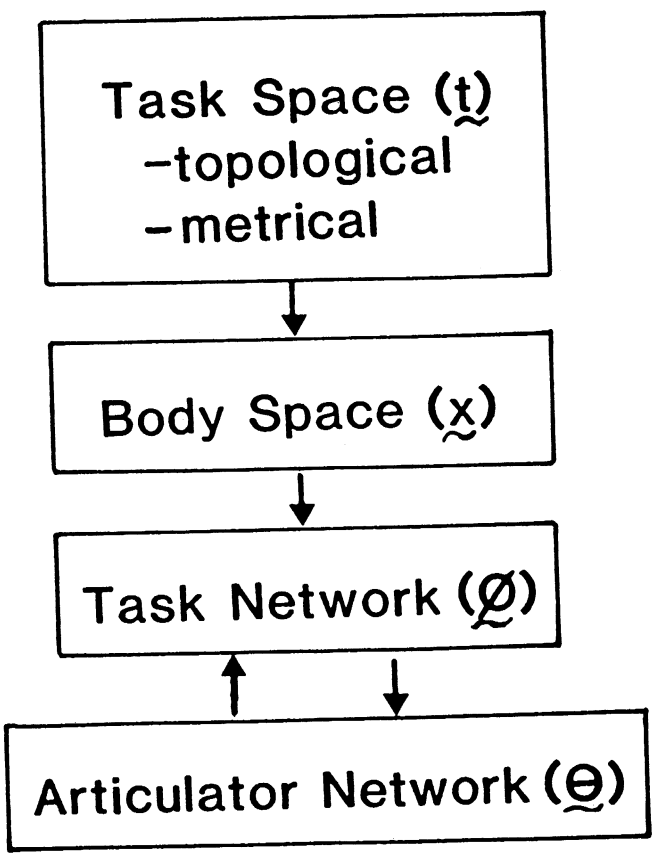

Figure 3. Overview of descriptive levels in task-dynamic approach.

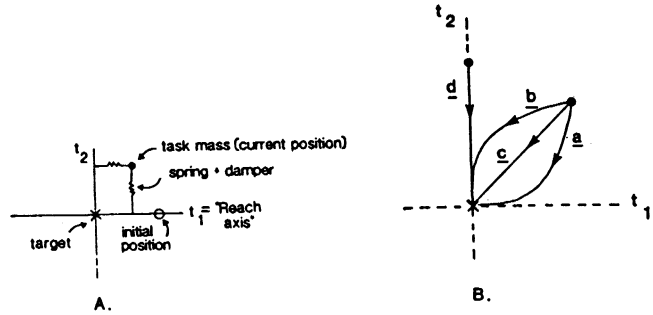

Figure 4. Task space descriptions of discrete reaching (A: Task space dynamics; B: system trajectories corresponding to different task axis weightings and initial conditions).

Two nested structures of constraint are defined at the task-space level. The first is defined globally and serves to establish a task-specific dynamical topology. In our reaching example, these global constraints specify point-attractor topologies along each task axis by establishing certain relations among the task-dynamic parameters (M_T, B_T, K_T). Additionally, a set of local constraints establish specific values for (i.e., tune) these parameters according to current task demands. Thus, in the reaching example m_T designates the perceptually estimated mass of the terminal device (i.e., gripper + any grasped object-to-be-moved), and B_T and K_T are specified according to the desired or required *damping ratios* ($\zeta_{Ti} = b_{Ti}/[2\sqrt{(m_Tk_{Ti})}]$; $i = 1, 2$) and *settling times* ($T_{si} = 4/[\zeta_{Ti}\sqrt{(k_{Ti}/m_T)}]$; $i = 1, 2$; i.e., the time required for the system to settle within 2% of the target amplitude; Dorf, 1974) along each task axis.

Movements of the task mass in reaching space display two properties that characterize the motions of terminal devices in real-world reaching tasks. Owing to the point-attractor dynamics, the task mass exhibits *equifinality* and will come to rest at

[6] Mason (1981; see also Raibert & Craig, 1981) has formalized a related geometrical description for manipulator contact tasks in which different tasks are characterized by distinct generalized surfaces in a constraint space. In this task-specific constraint space, the degrees of freedom are partitioned into those associated with either position or contact force control, respectively, during performance of the associated task. Such an approach requires, however, explicit task-specific and context-specific position and force trajectory plans for the task's terminal device. In contrast, the task-dynamic approach requires no such explicit trajectory plans, and task-appropriate trajectories for the terminal device emerge as implicit properties of the underlying task-dynamic regimes.

the target regardless of initial position (i.e., by definition, initial distance along t_1) and velocity (i.e., initial direction and speed of task space motion) and despite transient perturbations introduced en route to the target. Additionally, the task mass shows *straight line trajectories* during *un*perturbed motions, because in this case the system is effectively one-dimensional by virtue of the definition of the reach axis. However, motions in which the task mass is perturbed away from the reach axis will display trajectory shapes that depend on both the position in task space where the perturbation deposits the task mass and the relative values of k_{T_1} and k_{T_2} (assuming equivalent damping properties along each axis). As shown in Figure 4B, if one assumes critical damping along both task axes (i.e., $\zeta_{Ti} = 1.0$; $i = 1, 2$) and a postperturbation velocity of zero, then (a) when $k_{T_1} < k_{T_2}$, the task mass will approach the reach axis faster than axis t_2; (b) when $k_{T_1} > k_{T_2}$, the task mass will approach axis t_2 faster than t_1; and (c) when $k_{T_1} = k_{T_2}$, the task mass will approach t_1 and t_2 at the same speed and show a straight line postperturbation trajectory to the target. Such a trajectory will also result if, regardless of the relative values of k_{T_1} and k_{T_2}, the task mass is deposited precisely on the t_2 axis (Figure 4B, trajectory *d*). The reason for these relationships between perturbed position, relative axis stiffness, and trajectory shape lies in the shape of the potential energy functions that correspond to these different relative values of k_{T_1} and k_{T_2} (see Hogan, 1980, for a more detailed discussion of potential energy functions and spring stiffnesses in a similar two-dimensional mass-spring system). Finally, note that these free and perturbed trajectories evolve as implicit consequences of time-invariant task dynamics and require neither explicit trajectory plans nor replanning procedures.

Body space. The above time-invariant task-space regimes are defined relative to an abstractly defined goal location and a terminal device that was independent of any particular effector system. In order for these dynamical regimes to be useful to a performer, they must first be transformed into egocentric or body-space form (e.g., Saltzman, 1979). In contrast to task-space regimes, the body-space dynamics are specific to the particular effector system used to perform the task. Therefore, the transformation from task space to body space must be sensitive to the current spatial relationship between the performer's effector system and the task space. As illustrated in Figure 5A for a reaching task, this requirement corresponds to locating and orienting the task space relative to a body-space (x_1, x_2) coordinate system whose origin corresponds to the current location of the shoulder's rotation axis. The terminal device is a phantom hand that is considered to be disembodied from its effector system and is the body-space counterpart of the task mass in task space. Its current location is specified in x_1, x_2 coordinates. The set of local constraints given by the spatial relationship between task and body spaces serve to establish specific values for the body-space dynamic parameters $\mathbf{x}_0 = (x_{01}, x_{02})^T$ (the location of the task-space origin in body-space coordinates) and Φ (the orientation angle between the task space's reach axis t_1 and body-space axis x_1). (In these and the following expressions, a superscript T denotes the vector/matrix transpose operation.) Given this tuning information for $\mathbf{x}_0$ and Φ, the effector-independent task-space regime can be transformed into a corresponding effector-specific body or shoulder space regime. The resulting set of linear time-invariant body-space equations

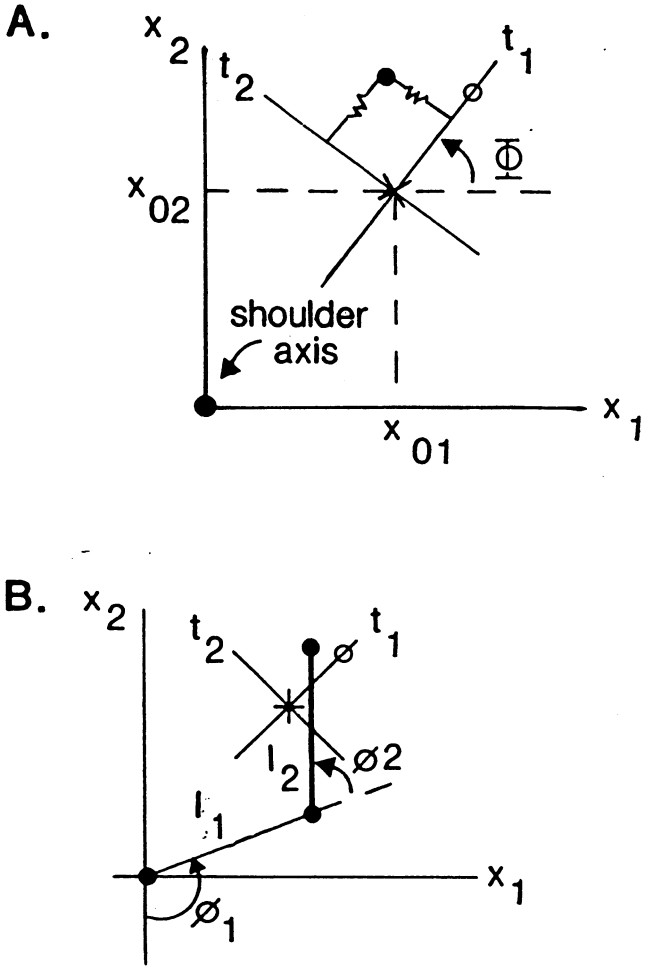

Figure 5. Discrete reaching. (A: body space. Task space is embedded in a shoulder-centered coordinate system. B: task network. Body space description is transformed into joint variable form of massless model arm.)

of motion for the terminal device are defined in matrix form as follows:

$$M_B\ddot{\mathbf{x}} + B_B\dot{\mathbf{x}} + K_B\Delta\mathbf{x} = \mathbf{0}, \tag{6}$$

where $M_B = M_T R$, M_T = task-space mass matrix; and

R = the rotation transformation matrix with elements r_{ij} converting task-space variables into body-space form;

$$= \begin{bmatrix} \cos\Phi & \sin\Phi \\ -\sin\Phi & \cos\Phi \end{bmatrix};$$

$B_B = B_T R$, where B_T = task-space damping matrix;

$K_B = K_T R$, where K_T = task-space stiffness matrix;

$\Delta\mathbf{x} = \mathbf{x} - \mathbf{x}_0$, where $\mathbf{x} = (x_1, x_2)^T$, the current body-space position vector of terminal device; and

$\mathbf{x}_0 = (x_{01}, x_{02})^T$, the body-space position vector of the task-space origin.

Equation 6, unlike Equations 4 and 5, represents a set of (usually) coupled equations of motion (i.e., the off-diagonal terms are generally nonzero owing to the rotation transformation).

However, as in Equations 4 and 5, the terms of Equation 6 are defined in force units, and its set of dynamic parameters is constant.

Joint variables and the task-dynamic network. The body-space dynamical regime is defined with reference to motions of an abstract terminal device disembodied from its effector system. This regime can be further transformed into an equivalent system based on the joint variables of a massless model effector system. Like the transformation from task space to body space, this transformation is strictly kinematic. It involves only the substitution of variables defined in one coordinate system for variables defined in another coordinate system. As illustrated in Figure 5B, this corresponds to expressing body-space variables ($\mathbf{x}, \dot{\mathbf{x}}, \ddot{\mathbf{x}}$) as functions of a model arm's kinematic variables ($\phi, \dot{\phi}, \ddot{\phi}$; where $\phi = [\phi_1, \phi_2]^T$, with ϕ_1 = shoulder angle defined relative to axis x_2, ϕ_2 = elbow angle defined relative to the upper arm segment). It should be emphasized that the model arm used in this transformation is defined in kinematic terms only (i.e., the proximal and distal segments have lengths l_1 and l_2, respectively, but no masses) and that the arm's proximal (shoulder) and distal (wrist) ends are attached to the body-space origin and the terminal device, respectively. The transformed equation (see Appendix for details) is as follows:

$$M_B J\ddot{\phi} + B_B J\dot{\phi} + K_B \Delta\mathbf{x}(\phi) = -M_B V\dot{\phi}_p, \qquad (7)$$

where M_B, B_B, K_B are the same constant matrices used in Equation 6;

$$\Delta\mathbf{x}(\phi) = \mathbf{x}(\phi) - \mathbf{x}_0,$$

where $\mathbf{x}(\phi) = [x_1(\phi), x_2(\phi)]^T$, the current body-space position vector of the terminal device expressed as a function of current joint angles;

$\mathbf{x}_0$ = the same constant vector used in Equation 6;

$J = J(\phi)$, the *Jacobian* transformation matrix whose elements J_{ij} are partial derivatives, $\partial x_i/\partial\phi_j$, evaluated at the current ϕ;

$\dot{\phi}_p = (\dot{\phi}_1^2, \dot{\phi}_1\dot{\phi}_2, \dot{\phi}_2^2)^T$, the current joint velocity product vector; and

$V = V(\phi)$, a matrix of coefficients associated with $\dot{\phi}_p$ introduced during the kinematic transformation and evaluated at the current ϕ.

The matrix products in Equation 7 are not constant but are nonlinearly dependent on the current posture ϕ of the arm model via the configuration dependence of the $J(\phi)$ and $V(\phi)$ matrices. Further, although Equation 7 is expressed in terms of articulator or effector system variables, it is by no means an articulator-dynamic equation. Rather, it is simply the body-space equation of motion (Equation 6) rewritten in the articulator-kinematic variables of a massless arm model. There is no reference as yet to the actual mechanics of a performer's corresponding real arm. The terms of Equation 7 are, in fact, still defined in units of force, not torque. Thus, if the initial state (ϕ_1, $\dot{\phi}_1$) for the model arm in Equation 7 specifies an initial body-space position and velocity for the model hand that is equal to the initial position and velocity for the phantom hand in Equation 6, then the model arm's joint angles will simply change (via Equation 7) in such a way that the model hand moves along exactly the same trajectory as would the phantom hand (via Equation 6).

Equation 7 may be rewritten in units of angular acceleration:

$$\ddot{\phi} + J^{-1}M_B^{-1}B_B J\dot{\phi} + J^{-1}M_B^{-1}K_B\Delta\mathbf{x}(\phi) + J^{-1}V\dot{\phi}_p = \mathbf{0} \qquad (8)$$

In effect, this equation describes a network of task- and context-specific dynamical relations among the model arm's articulator-kinematic variables. Consequently, we consider Equation 8 to define the so-called task-dynamic network (*task network*) for our reaching example. Ultimately, however, a reaching task is performed by a real arm whose unperturbed motions and responses to perturbations are shaped according to task-specific, evolving constraints on the articulator-dynamic parameters. In our task-dynamic modeling, such constraints originate in the task-network equation (Equation 8).

We now review the basic articulator dynamics of a simple two-jointed arm and then discuss two alternative ways in which Equation 8 might be used to constrain these dynamics for a reaching task.

Articulator Dynamics and the Articulator Network

For the purpose of simplicity, we restrict our discussion to a two-joint, two-segment effector system whose segments ("upper arm" and "forearm") have lengths l_1 and l_2, with masses m_1 and m_2 uniformly distributed along the respective segment lengths. Assuming frictionless revolute joints (θ_1, θ_2; defined in the same manner as for the model arm) and no gravity, the passive mechanical (no controls) equation of motion for this "real" arm (see Appendix for details) is as follows:

$$M_A\ddot{\theta} + S_A\dot{\theta}_p = \mathbf{0}, \qquad (9)$$

where $M_A = M_A(\theta)$, the 2×2 *acceleration sensitivity matrix* associated with inertial torques, whose elements are functions of the current linkage configuration, θ; The subscript A denotes articulator-dynamic elements;

$S_A = S_A(\theta)$, a 2×3 matrix associated with coriolis torques (related to joint velocity cross products) and centripetal torques (related to squares of joint velocities), whose elements are functions of the current linkage configuration, θ.

With controls included, this equation becomes

$$M_A\ddot{\theta} + S_A\dot{\theta}_p + B_A\dot{\theta} + \tau_{As} + \tau_{Aa} = \mathbf{0}, \qquad (10)$$

or

$$K_A\Delta\theta$$

where B_A = a 2×2 control damping matrix;

τ_{As} = a 2×1 control spatial-spring torque vector;

K_A = a control 2×2 joint-stiffness matrix;

$\Delta\theta = \theta - \theta_0$, where θ_0 = a 2×1 control reference-configuration vector; and

τ_{Aa} = a 2×1 control additional torque vector, whose function will be described more fully in the following section on control laws.

The terms of Equations 9 and 10 are defined in units of torque. Equation 10 can be rewritten in units of angular acceleration:

$$\ddot{\theta} + M_A^{-1}B_A\dot{\theta} + M_A^{-1}\tau_{As} + M_A^{-1}S_A\dot{\theta}_p + M_A^{-1}\tau_{Aa} = 0. \quad (11)$$

or

$$M_A^{-1}K_A\Delta\theta$$

Just as Equation 8 was considered to define a network of task-dynamical relations for a kinematic arm model, Equation 11 can be considered to define a network of articulator-dynamic relations (*articulator network*) among the real arm's joint variables.

For our reaching example (and other real-world tasks as well), the question at this point becomes the following: How can patterns of control parameters be specified over time for the real arm (the articulator-dynamic controls in Equations 10 and 11) so that it will behave identically or nearly identically to the model arm (Equations 7 and 8)? In the sections below we consider two related methods based on alternate versions of Equation 11. The first method (control law) uses Equations 8 and 11 to formulate task-specific equations of constraint or control laws over the articulator-dynamic parameters; the second method (network coupling) combines the use of control laws with the concept of coupling between the task (Equation 8) and articulator (Equation 11) networks. Both methods are applicable to the coordination and control of movements in artificial linkage systems (e.g., robotic, prosthetic). The network coupling method also affords a novel perspective on motor control in physiological systems. In the following section, the control law method is described. Network coupling will be discussed in a later section on physiological modes of motor control.

Method 1: Control Laws

This method is conceptually quite simple and is outlined in Figure 6. First, the model arm state (ϕ, $\dot{\phi}$) is assumed to equal the real arm state (θ, $\dot{\theta}$), and θ and $\dot{\theta}$ (hence, also, ϕ and $\dot{\phi}$) are assumed to be specified proprioceptively. Second, the following version of Equation 11 is used:

$$\ddot{\theta} + M_A^{-1}B_A\dot{\theta} + M_A^{-1}\tau_{As} + M_A^{-1}S_A\dot{\theta}_p + M_A^{-1}\tau_{Aa} = 0 \quad (12)$$

Third, by comparing Equations 8 and 12 and recalling that $\phi = \theta$ and $\dot{\phi}_p = \dot{\theta}_p$ by assumption, one can see that the real arm (θ variables) will move according to task-dynamic requirements (i.e., will move identically to the model arm [ϕ variables]) when the following identities hold: (a) $J^{-1}M_B^{-1}B_BJ = M_A^{-1}B_A$, (b) $J^{-1}M_B^{-1}K_B\Delta x(\theta) = M_A^{-1}\tau_{As}$, and (c) $J^{-1}V\dot{\theta}_p = M_A^{-1}S_A\dot{\theta}_p + M_A^{-1}\tau_{Aa}$. Finally, these identities are used to define the following nonlinear, state-dependent control laws for the articulator-dynamic parameters:

$$B_A = M_AJ^{-1}M_B^{-1}B_BJ; \quad (13)$$

$$\tau_{As} = M_AJ^{-1}M_B^{-1}K_B\Delta x(\theta); \quad (14)$$

$$\tau_{Aa} = (M_AJ^{-1}V - S_A)\dot{\theta}_p. \quad (15)$$

The articulator-dynamic controls in Equations 13, 14, and 15 are defined by the linkage configuration (θ)-dependent or state (θ, $\dot{\theta}$)-dependent products of (a) M_A, S_A, J, J^{-1}, V, $x(\theta)$, and $\dot{\theta}_p$ (these terms are functions of θ or $\dot{\theta}$ but are task independent)[7] and (b) M_B^{-1}, B_B, K_B, and x_0 (these are constant but depend on both spatial context and task).

For purposes of simplicity we have assumed that the computations involved in Equations 13–15 occur instantaneously. However, in reality this cannot be the case, and there must be a delay (Δt) between sensing a given linkage state (at $t = t_i$) and specifying a task- and context-specific set of controls (at $t = t_i + \Delta t$). It is possible, therefore, that these controls will be totally inappropriate for the current ($t = t_i + \Delta t$) linkage state. There are two main ways to deal with this problem. The first is to minimize Δt by using a variety of methods: (a) table look up (e.g., Raibert, 1978) for those terms in Equations 13–15 that are independent of the current spatial and task contexts but can be indexed according to current articulatory state; (b) parallel computation procedures, such that all elements in all matrices in Equations 13–15 are not computed sequentially; (c) computation strategies that heuristically omit certain terms in Equations 13–15[8] or that capitalize on the repeated use of certain "modular" functions (e.g., Benati, Gaglio, Morasso, Tagliasco, & Zaccaria, 1980) in the equations' component terms; and/or (d) use of remote sensing (exproprioception, e.g., vision) to specify certain information directly (e.g., hand position x) rather than indirectly through computations based on proprioceptive feedback (e.g., x[θ]). The second way of reducing the adverse effects of delays is to use a predictive, "look-ahead" type of computation (e.g., Ito, 1982; Pellionisz & Llinas, 1979), such that given an estimate of delay Δt, the system might sense a linkage state at $t = t_i$, predict the state at $t = t_i + \Delta t$, and perform the equations' computations with reference to this predicted state.

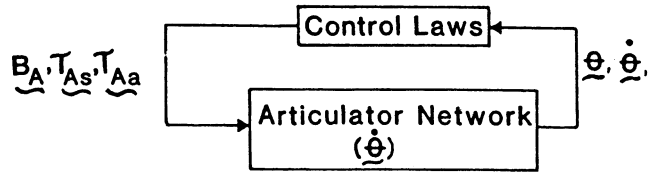

Figure 6. Overview of information flow in control law version of task dynamics.

[7] In redundant task-articulator situations (see Footnote 3), J^{-1} is not defined and the Jacobian pseudoinverse (J^+) or weighted Jacobian pseudoinverse (J^*) may be used (Benati et al., 1980; Klein & Huang, 1983; Whitney, 1972). Using J^* provides an optimal weighted least squares solution for the differential transformation from spatial to joint motion variables. If this weighting is task dependent, then J^* would be both task and configuration dependent. For example, if a three-joint arm is used to position the fingertip in a spatially planar reaching task, different weightings would correspond to different arm joint motion strategies. One weighting might correspond to a predominantly shoulder motion strategy, whereas a second weighting might specify a predominantly elbow motion strategy, and so on. In such cases, elements of the weighting matrices used for the corresponding weighted Jacobian pseudoinverses define a further set of tuning parameters for the task network Equation 11.

[8] As we demonstrate via simulation (in the *Trajectory Shaping* section) for a task-space point attractor in our reaching example, it may be possible to ignore the velocity product torque terms and therefore omit τ_{Aa} from Equation 12. In these cases, the system still arrives at the desired target via quasi-straight-line hand trajectories. In fact, reach trajectories generated without such corrections appear more similar to experimentally observed trajectories than ones generated with "perfect" velocity product torque corrections.

Further Examples

In the preceding sections we described the control law version of the task-dynamic model in the context of the point-attractor topology associated with a discrete reaching task. In the present section, we generalize this approach to other task types as well as to variations of the discrete reaching task. Specifically we describe how task dynamics (a) generates task-specific trajectory shapes in discrete reaching, rhythmic target-to-target, cup-to-mouth, and crank-turning tasks and (b) provides "immediate compensation" to a sustained perturbation introduced to an effector system while en route to a target in a reaching task.

All examples and computer simulations are described below in the current control law context and represent motions of the (simplified) real arm. The model arm is rigidly constrained to move identically to the real arm, owing to the assumptions that $\phi = \theta$ and $\dot{\phi} = \dot{\theta}$, given the current proprioceptively specified θ and $\dot{\theta}$.

Trajectory Shaping

Discrete reaching. This is the by-now familiar example of discrete reaching whose task space is defined as a two-dimensional point attractor (see Figure 4A). Figure 7 (trajectory *a*) shows a straight-line trajectory for the terminal device (the hand) that is generated by these task dynamics. For this trajectory the stiffnesses of the task-space axes are symmetrical (i.e., $k_{T_1} = k_{T_2}$), and critical damping is assumed along both axes. Note, however, that perfect straight-line trajectories are generated in contrast to the quasi-straight-line trajectories observed experimentally for primates (e.g., Georgopoulos, Kalaska, & Massey, 1981; Morasso, 1981; Soechting & Lacquaniti, 1981).

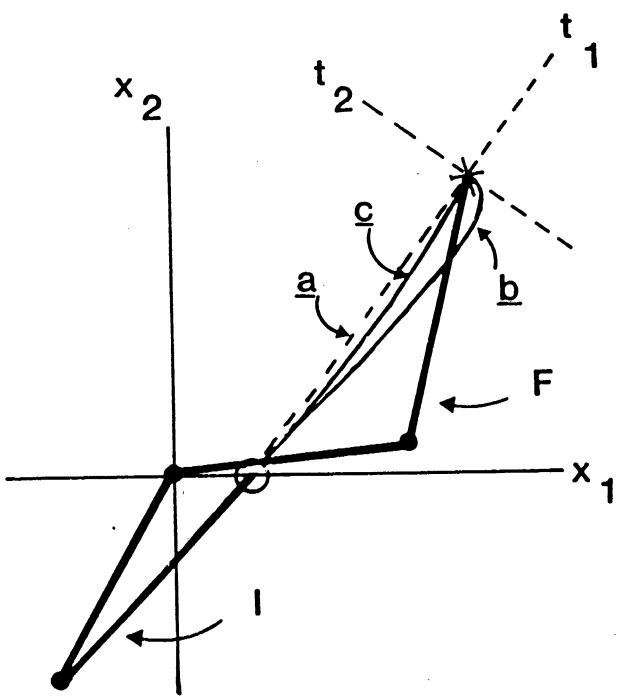

Figure 7. Body-space discrete reaching trajectories showing effects of omitting velocity product torque compensation terms with different task axis weightings. (*I* and *F* denote initial and final arm configurations, respectively.)

As alluded to earlier (see also Footnote 8), it is possible to omit τ_{A_a} (i.e., the control vector associated with velocity product torques) from Equation 12. As a result, more "realistic" trajectories are generated (trajectory *b* in Figure 7), and at the same time, the amount of computation involved in specifying the articulator-dynamic controls is reduced. As with trajectory *a*, trajectory *b* shows a reach involving symmetrical task axis stiffnesses and critical task-space damping. Omitting τ_{A_a} results in an articulator network equation whose velocity product terms are simply those of the arm's passive mechanics (i.e., $S_A\dot{\theta}_p$ in Equation 9) rather than those specified by the task network equation (i.e., $M_B V\dot{\phi}_p$ in Equation 7). Although the omission of τ_{A_a} introduces a hook into trajectory *b*'s illustrated hand motion, the hand nevertheless arrives precisely on target because of the underlying point-attractor dynamics in the task space. This preservation of accurate targeting behavior when control terms related to velocity product torques are ignored is a feature of the task-dynamic approach not shared by some other robotic control schemes (e.g., Hollerbach & Flash, 1981, see their Figure 8). Straight-line hand trajectories can be approximated when τ_{A_a} is omitted, however, by a judicious relative weighting of task axis stiffnesses. Hand trajectories progressively closer to ideal straight lines will be produced using progressively greater penalties for task mass deviations from the task-space reach axis (t_1) while en route to the target. A hand trajectory for the arm motion corresponding to one such ratio (k_2:k_1 = 1.75:1) with critical damping along both task axes is shown in Figure 7 (trajectory *c*).

Cup-to-mouth task. In a cup-to-mouth task, the goal is to move a cup of liquid from an initial to a final position (e.g., table top to mouth) while maintaining a horizontal spillage-preventing cup orientation during the movement. As in our discussion of the discrete reaching task, we begin with a simplified task-dynamic treatment of a planar cup-to-mouth task performed by a three-joint arm (shoulder, elbow, wrist) using an abstract, functional description of that skill's task space. This task space is modeled as a point attractor in three dimensions (one rotational and two linear degrees of freedom) and is shown in Figure 8A. In this figure the terminal device is an abstract task segment (m_T = mass, l_T = length) representing the grasped cup, with one end (the distal end) defined as the point of final cup–mouth contact. The task segment requires three coordinates for its complete task-space description. The target location (mouth) for the segment's distal end defines the origin (t_{01}, t_{02}) of a t_1t_2 Cartesian coordinate system; axis t_1 is defined as a reach axis from the initial position of the segment's distal end to the t_1t_2 origin; axis t_2 is defined orthogonally to t_1. The orientation of the task segment relative to axis t_1 defines the current angular t_3 coordinate; t_{03} defines the (identical) initial and target task-segment orientations; and $I_T(=[1/3]m_T l_T^2)$ is the task segment's moment of inertia about its distal end. The equations of motion corresponding to axes t_1, t_2, and t_3 are

$$m_T\ddot{t}_1 + b_{T_1}\dot{t}_1 + k_{T_1}t_1 = 0; \tag{16}$$

$$m_T\ddot{t}_2 + b_{T_2}\dot{t}_2 + k_{T_2}t_2 = 0; \tag{17}$$

$$\rho I_T\ddot{t}_3 + \rho b_{T_3}\dot{t}_3 + \rho k_{T_3}(t_3 - t_{03}) = 0. \tag{18}$$

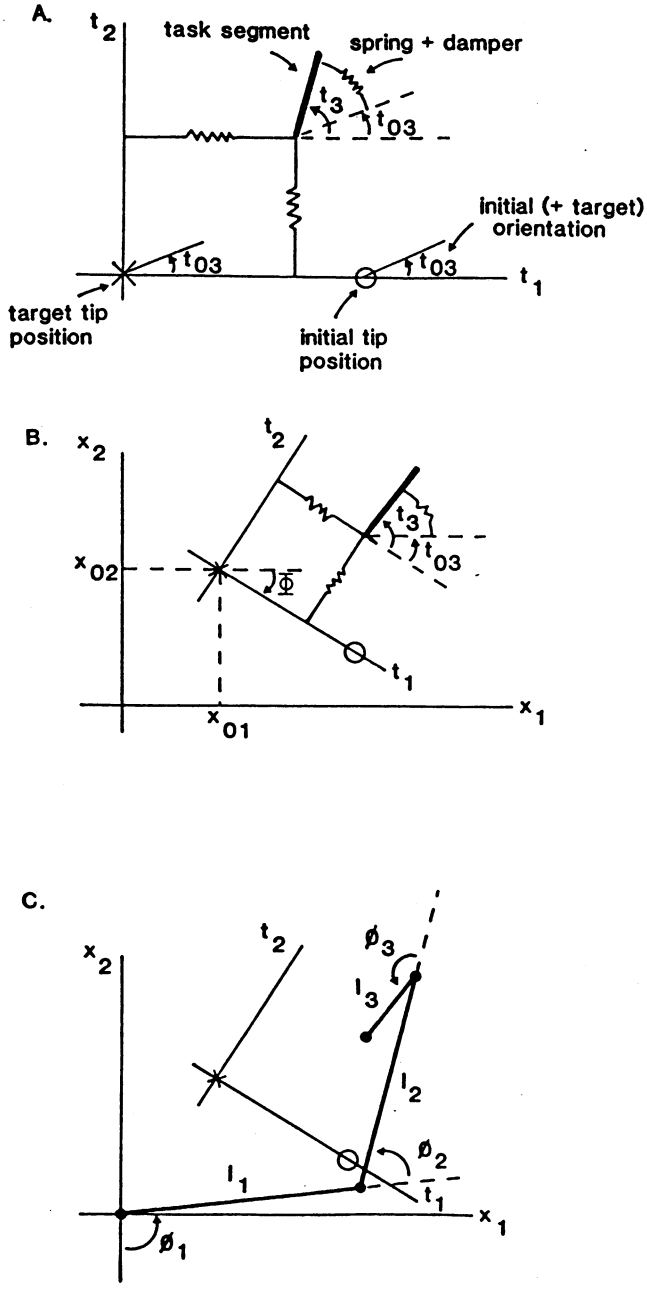

Figure 8. Cup-to-mouth task (A: task space; B: body space; C: task network).

In Equations 16–18, ρ is a constant scaling factor with units of length and is used to ensure dimensional homogeneity along all task-space degrees of freedom. Thus, all terms of Equations 16–18, even the rotational terms of Equation 18, are defined in units of force. For purposes of the present article, ρ is set to 1 and is consequently omitted for notational simplicity in all further discussions in this section.[9] In Figure 8A the stiffness and damping elements are represented in lumped form as squiggles in the lines connecting the task segment to the linear rest positions and to the rotational rest orientation. Equations 16–18 describe a set of uncoupled (by definition of the abstract task space) equations with constant parameters and can be represented in matrix form as

$$M_T\ddot{t} + B_T\dot{t} + K_T\Delta t = 0, \tag{19}$$

where M_T, B_T, and K_T are 3 × 3 diagonal matrices of task-dynamic parameters analogous to the simpler 2 × 2 point-attractor system of Equation 5. In a similar fashion, the body-space equation and the model arm (task network) equation are simply the 3 × 3 analogs of Equations 6 and 8. The corresponding body-space and model arm representations are illustrated in Figures 8B and 8C.

When simulated, a typical movement generated by these task dynamics, using symmetrical task axis stiffnesses ($k_{T_1} = k_{T_2} = k_{T_3}$) and critical damping along all task axes, shows both a straight-line trajectory and a maintained horizontal orientation of the task segment during the movement.

Reaching (rhythmic). The point-attractor topologies in the task space that are used for the discrete reaching and cup-to-mouth tasks are unable to generate sustained cyclic hand motions between two body spatial targets. Consider, for example, the case of planar motion of the terminal device (hand) and a corresponding two-joint effector system (arm with shoulder and elbow joints). The task space is illustrated in Figure 9A and consists of an orthogonal pair of axes (t_1, t_2) for which (a) t_1 is defined along the line between the two targets (D = distance between the targets) and (b) the origin is located midway between the two targets ($A = D/2$ = distance from origin to either target). The terminal device is an abstract point task mass (m_T = mass) and may be located anywhere in the task space. Point-attractor dynamics are defined along axis t_2 to bring the task mass onto axis t_1 and to maintain it there despite transient perturbations introduced perpendicular to t_1. Limit cycle (periodic attractor) dynamics are defined along axis t_1 to sustain a cyclic motion of the task mass parallel to t_1 between the two targets and to maintain the desired oscillation amplitude ($A = D/2$) despite perturbations introduced parallel to t_1. The task-space equations of motion are

$$m_T\ddot{t}_1 - b_{T_1}\dot{t}_1 + c_{T_1}t_1^2\dot{t}_1 + k_{T_1}t_1 = 0; \tag{20}$$

$$m_T\ddot{t}_2 + b_{T_2}\dot{t}_2 + k_{T_2}t_2 = 0, \tag{21}$$

where m_T, k_{T_1}, b_{T_2}, and k_{T_2} are defined as in Equation 5 (discrete reaching task, point attractor) and $(-b_{T_1}\dot{t}_1 + c_{T_1}t_1^2\dot{t}_1)$ is the nonlinear escapement term (van der Pol type) for axis t_1.

The dynamic parameters for axis t_2 are tuned in the same manner as for the t_2 axis of the discrete reach task space (see earlier section on task space). Tuning the dynamic parameters for axis t_1 involves specifying k_{T_1} according to the desired period, P, of motion and the relation $P = 2\pi/\sqrt{(k_{T_1}/m_T)}$. The

[9] The desirability of using such scaling coefficients was pointed out by Mason (1981). In addition to ensuring dimensional homogeneity, Mason showed that they could be used to differentially weight the strength of control along the rotational and linear dimensions of task performance. However, because the task-dynamic approach uses relative task axis stiffness weightings for this purpose, the value of ρ was simply set to 1.0 in our treatments.

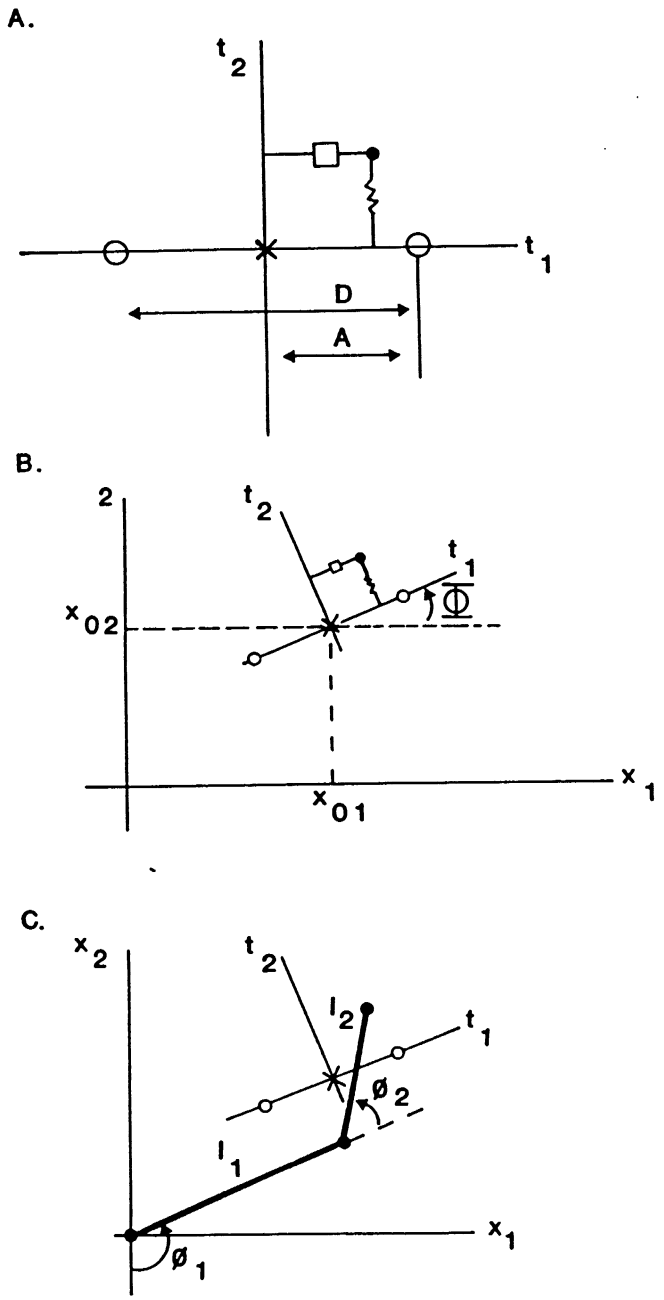

Figure 9. Rhythmic reaching. (A: task space. Open circles represent targets; squiggle represents point-attractor [spring and damper] dynamics along axis t_2; open box represents limit cycle [spring and van der Pol escapement] dynamics along axis t_1. B: body space. C: task network.)

procedure for specifying b_{T_1} and c_{T_1} is more involved and may be understood by rewriting Equation 20 in the following normalized, dimensionless form:

$$Z_1'' - \epsilon(1 - Z_1^2)Z_1' + Z_1 = 0, \tag{22}$$

where (a) the single and double apostrophe superscripts denote differentiation with respect to the dimensionless time variable, $N = \omega_0 n$, with $\omega_0 = \sqrt{(k_{T_1}/m_T)}$ and n being the standard time variable; (b) $Z_1 = \sqrt{(c_{T_1}/b_{T_1})}t_1$ is the dimensionless displacement variable; and (c) $\epsilon = b_{T_1}/\sqrt{(m_T k_{T_1})}$ is a dimensionless measure directly related to both escapement strength (i.e., the strength with which the system resists being displaced from the limit cycle) and the shape of the limit cycle orbit in the phase plane (e.g., $\epsilon \ll 1$ corresponds to a circular orbit and sinusoidal motion; $\epsilon \gg 1$ corresponds to a relaxation orbit and a steplike motion). Given values for k_{T_1} (from the desired period) and ϵ (from the desired orbit shape), b_{T_1} is determined from the above expression for ϵ. Finally, it is known that the amplitude for the normalized (Z variable) system of Equation 22 is equal to 2.0 over a wide range of ϵ values (e.g., $0 \leq \epsilon \leq 10$; Jordan & Smith, 1977). For the original nonnormalized (t variable) system of Equation 20, the corresponding amplitude is $A = 2\sqrt{(b_{T_1}/c_{T_1})}$. Therefore, given values for b_{T_1} and desired amplitude A, the value of c_{T_1} is determined from the preceding expression for A. Finally, Equations 20 and 21 may be rewritten in matrix form as

$$M_T\ddot{\mathbf{t}} + B_T\dot{\mathbf{t}} + K_T\mathbf{t} = \mathbf{F}_T, \tag{23}$$

where M_T and K_T are defined as in Equation 5;

$B_T = \begin{bmatrix} -b_{T_1} & 0 \\ 0 & b_{T_2} \end{bmatrix}$, denoting the linear damping components; and

$\mathbf{F}_T = (-c_{T_1}t_1^2\dot{t}_1, 0)^T$, denoting nonlinear system components.

Equations 20, 21, and 23 represent a time-invariant (autonomous), uncoupled, task-space dynamical system with constant parameters. Figure 9B illustrates how the task space is located and oriented in body (shoulder) space. The body-space dynamical system is described by

$$M_B\ddot{\mathbf{x}} + B_B\dot{\mathbf{x}} + K_B\Delta\mathbf{x} = \mathbf{F}_B, \tag{24}$$

where $M_B = M_T R$, where R = the rotational transform matrix with elements r_{ij} defined previously in Equation 6;

$B_B = B_T R$;

$K_B = K_T R$; and

$\mathbf{F}_B = (-c_{T_1}(r_{11}\Delta x_1 + r_{12}\Delta x_2)^2(r_{11}\dot{x}_1 + r_{12}\dot{x}_2), 0)^T$.

Equation 24 describes an autonomous, coupled (due to the rotation transformation), body-space dynamical system with a constant set of linear parameters and a nonlinear, state-dependent forcing function. This body-space equation can be transformed kinematically into joint variable form by expressing x variables as functions of the ϕ variables of a corresponding model arm (see Figure 9C):

$$M_B J\ddot{\phi} + B_B J\dot{\phi} + K_B\Delta\mathbf{x}(\phi) = \mathbf{F}_\phi - M_B V\dot{\phi}_p, \tag{25}$$

where M_B, B_B, and K_B are defined as in Equation 24;

$J = J(\phi)$, the Jacobian matrix;

$\Delta\mathbf{x}(\phi) = \mathbf{x}(\phi) - \mathbf{x}_0$;

$\mathbf{F}_\phi = \mathbf{F}_B(\phi)$, that is, $\mathbf{F}_B$ with the substitutions $\Delta x_1 = \Delta x_1(\phi)$, $\Delta x_2 = \Delta x_2(\phi)$, $\dot{x}_1 = J_{11}\dot{\phi}_1 + J_{12}\dot{\phi}_2$, $\dot{x}_2 = J_{21}\dot{\phi}_1 + J_{22}\dot{\phi}_2$; and

V and ϕ_p are as defined in Equation 7.

Equation 25 may be rewritten in the following task-network form:

$$\ddot{\phi} + J^{-1}M_B^{-1}B_B J\dot{\phi} + J^{-1}M_B^{-1}K_B\Delta x(\phi) = J^{-1}M_B^{-1}F_\phi - J^{-1}V\dot{\phi}_p. \quad (26)$$

Because the real arm's motion can be described by the articulator network (θ variables) Equation 12, the articulator controls B_A and τ_{As} are specified according to control laws 13 and 14, respectively. A comparison of equations 12 and 26 shows that, assuming $\phi = \theta$ and $\dot{\phi} = \dot{\theta}$, the articulator control τ_{As} is defined according to the following control law:

$$\tau_{As} = (M_A J^{-1}V - S_A)\dot{\phi}_p - M_A J^{-1}M_B^{-1}F_\phi. \quad (27)$$

A typical movement generated for the hand in body (shoulder) space is illustrated in Figure 10. Note the straight-line hand trajectory during the steady-state cyclic motion between targets and also the way the hand is attracted autonomously to this steady-state trajectory despite a start-up position (with zero velocity) away from this trajectory.

Crank turning. Figure 11C shows a crank-turning task in shoulder space for which (a) motion of arm and crank occur in the horizontal plane; (b) the crank segment's distal end is attached to a fixed rotation axis located at x_0 in shoulder space; (c) the crank rotates at a constant angular velocity, V, about the fixed axis; (d) the wrist joint is fixed and the hand tightly grasps the crank's handle, which freely rotates about an axis fixed to the crank's proximal end; and (e) ϕ_1 and ϕ_2 represent the shoulder and elbow angles, respectively, and ϕ_3 represents the angle between the hand–forearm and crank. The task space description is illustrated in Figure 11A, in which (a) the crank is the terminal device or task segment (m_T = mass, l_T = length); (b) the fixed rotation axis at the crank's distal end defines the origin of a Cartesian t_1t_2 coordinate system; (c) an angular t_3 coordinate is defined by the orientation of the crank relative to axis t_1; and (d) $I_T = (1/3)m_T l_T^2$ is the crank's moment of inertia about its distal end. The task-space equations of motion are defined as

$$m_T\ddot{t}_1 + b_{T_1}\dot{t}_1 + k_{T_1}t_1 = 0; \quad (28)$$

$$m_T\ddot{t}_2 + b_{T_2}\dot{t}_2 + k_{T_2}t_2 = 0; \quad (29)$$

$$\rho I_T\ddot{t}_3 - \rho b_{T_3}\dot{t}_3 + \rho c_{T_3}\dot{t}_3^3 = 0. \quad (30)$$

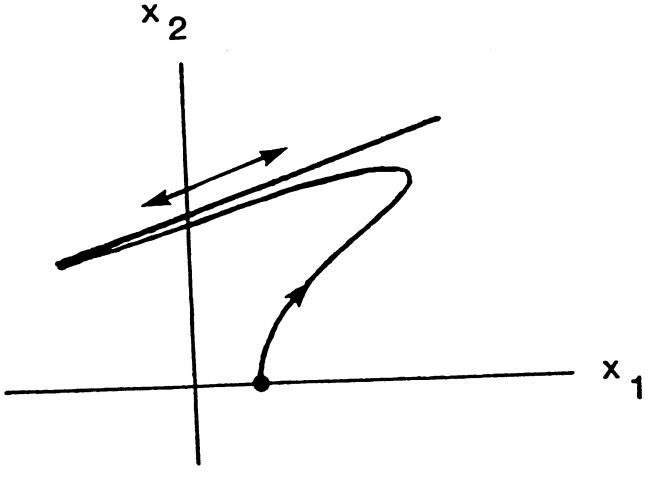

Figure 10. Body-space rhythmic reaching trajectory when hand starts (or is perturbed to) a position away from the steady state trajectory.

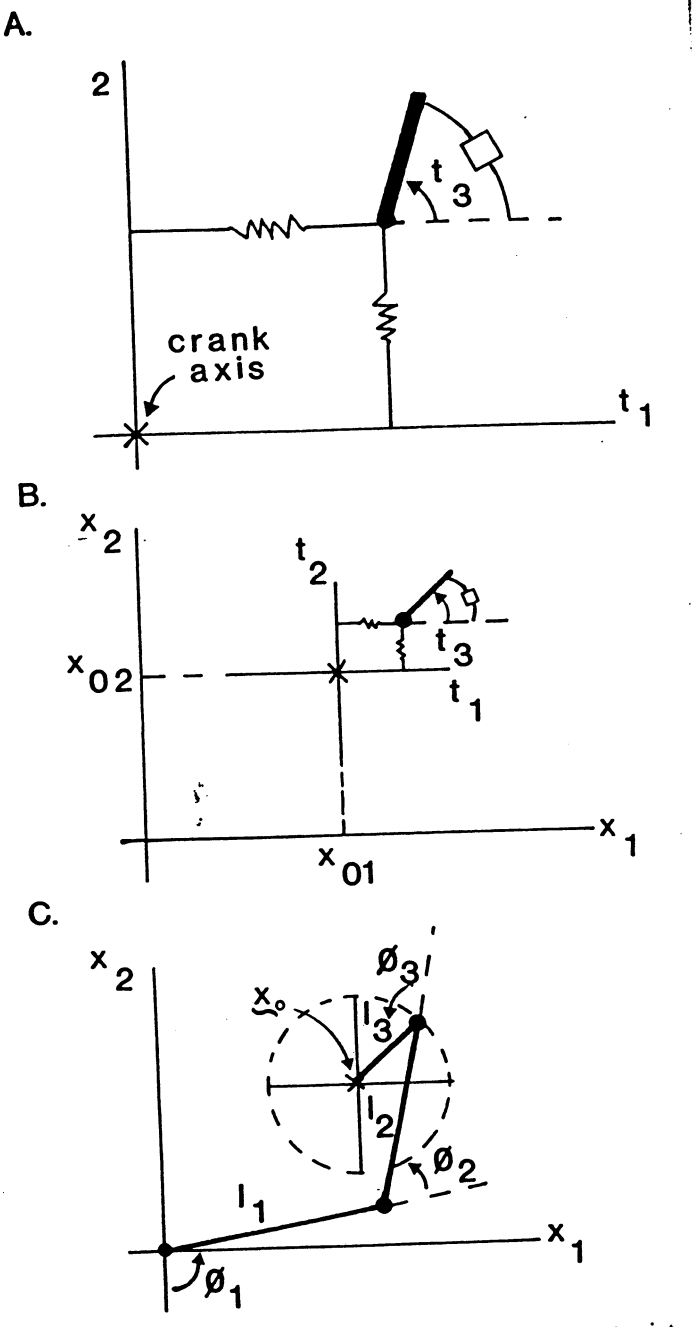

Figure 11. Crank turnings. (A: task space. Squiggles represent point-attractor dynamics along linear axes t_1 and t_2; open box represents velocity-attractor [Rayleigh escapement] dynamics along rotational axis t_3; B: body space. C: task network.)

In Equation 30, ρ is the same scaling factor used in Equation 18 and is omitted from further discussions in this section for notational simplicity.

Equations 28 and 29 define point attractors whose damping and stiffness elements are represented in lumped form in Figure 11A. These dynamics maintain the crank's distal end at the task-space origin. Because in the real world the crank is fixed to this axis, these axes may be weighted rather loosely (i.e., they

may be assigned low values for k_{T_1} and k_{T_2}). Equation 30 needs a bit more explanation. It contains a limit cycle's escapement term (Rayleigh type escapement: $-b_{T_3}\dot{t}_3 + c_{T_3}\dot{t}_3^3$) but no spring term. The behavior associated with Equation 30 is best understood by examining its corresponding phase portrait (Figure 12). Three steady states are represented by lines parallel to the t_3 axis. The lines defined by $\dot{t}_3 = \pm V = \pm\sqrt{(b_{T_3}/c_{T_3})}$ are stable steady states, and the line $\dot{t}_3 = 0$ denotes an unstable steady state. In other words, given any nonzero start-up velocity in either the upper or lower half plane, the system will reach the corresponding positive or negative steady-state angular velocity, $\pm V$. If, however, the system begins at any angular position with precisely zero velocity, it will simply stay at that position. In normalized form, Equation 30 becomes

$$\ddot{Z}_3 - \epsilon(1 - \dot{Z}_3^2)\dot{Z}_3 = 0, \tag{31}$$

where $Z_3 = \sqrt{(c_{T_3}/b_{T_3})}t_3$ is the dimensionless displacement variable, and $\epsilon = b_{T_3}/I_T$ is directly related to the strength of the escapement (i.e., the speed with which the system attains the steady state and the strength with which it resists perturbations from the steady state). Because we are unaware of any other label for this type of dynamical topology, we call it a *bistable velocity attractor* (or more simply, a *velocity attractor*). Given a desired escapement strength (ϵ) and final crank angular velocity (V), the above relationships are sufficient to tune the system's b_{T_1} and c_{T_1} values according to these task demands. Equations 28–30 can be rewritten in matrix form as

$$M_T\ddot{\mathbf{t}} + B_T\dot{\mathbf{t}} + K_T\mathbf{t} = \mathbf{F}_T, \tag{32}$$

where M_T is defined as in Equation 19;

$$B_T = \begin{bmatrix} b_{T_1} & 0 & 0 \\ 0 & b_{T_2} & 0 \\ 0 & 0 & -b_{T_3} \end{bmatrix}; \quad K_T = \begin{bmatrix} k_{T_1} & 0 & 0 \\ 0 & k_{T_2} & 0 \\ 0 & 0 & 0 \end{bmatrix}; \text{ and}$$

$$\mathbf{F}_T = (0, 0, -c_{T_3}\dot{t}_3^3)^T$$

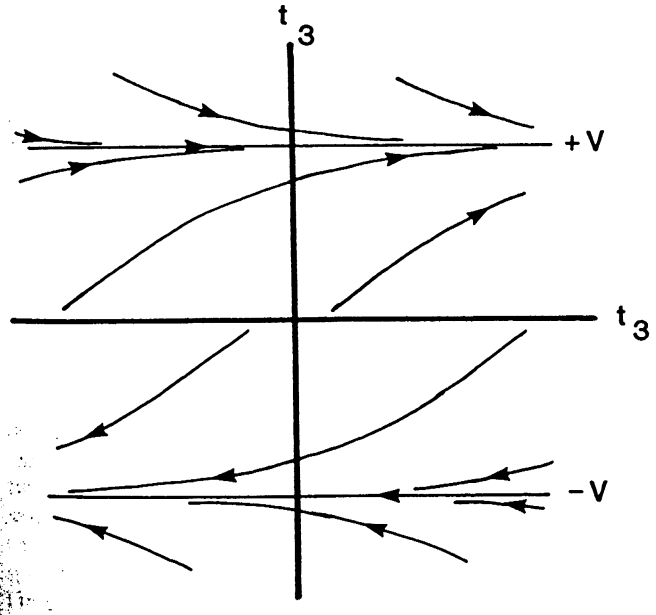

Figure 12. Phase portrait of velocity-attractor system.

Equations 28–30 and 32 represent a time-invariant (autonomous), uncoupled (by definition) task-space dynamical system with constant parameters. Figure 11B shows how the task space is located and oriented in body (shoulder)-space coordinates. The orientation of task space to body space is arbitrary, and in Figure 11B the orientation angle Φ is simply assumed to be 0 (e.g., see Figure 8B for an example of a different task with nonzero Φ). Figure 11C, as mentioned previously, shows the relation of the task and body spaces to the task's model arm. Equations for body-space and model-arm dynamics can be derived from Equation 32 in a mannar similar to that used in generating Equations 24, 25, and 26 from Equation 23.

The configuration ϕ of the model arm is specified in the following way. Angles ϕ_1 (shoulder) and ϕ_2 (elbow) can be obtained proprioceptively, but ϕ_3, the angle between the crank and the hand–forearm, cannot. However, assuming that the location of the crank's distal end (environmentally fixed rotation axis) is known in body-space coordinates and given ϕ_1 and ϕ_2 proprioceptively, ϕ_3 is uniquely specified by geometric considerations. Thus, the full ϕ set is available for use in the control law computations.

Immediate Compensation

In the introduction to this article, we reviewed experimental data on speech movements that showed task-specific patterns of compensatory responses in remote articulators to unpredicted transient perturbations in a given articulator. These compensations were relatively immediate and implied that selective patterns of coupling or gating existed among the component articulators that were specific to the produced utterances. In the context of task dynamics, we hypothesize that these coupling patterns are due to corresponding patterns of evolving articulator-dynamic controls that are specified by task- and state-dependent control laws.

To illustrate, consider the following example of a discrete reaching task (formulated as a modified version of a cup-to-mouth task) in which (a) the terminal device is a pointer fixed to the hand of a three-segment (upper arm, forearm, hand–pointer) arm; (b) planar motion of the pointer corresponds to angular motions of the arm's three joints (ϕ_1 = shoulder, ϕ_2 = elbow, ϕ_3 = angle between pointer and forearm); and (c) task demands emphasize positioning the pointer's distal end at a body-space x_1x_2 target but are relatively lenient regarding the precision of final orientation. Consequently, the task space is described as a three-dimensional point attractor with symmetrical weightings for the linear t_1 and t_2 axes and a much smaller weighting for the rotational t_3 axis. Figure 13 illustrates the initial (*a*) and final (*b*) arm configurations that correspond to these task dynamics (weighting ratio of axes t_1 and t_2 to t_3 is 20:1) when the arm encounters no perturbations en route to its target. The initial arm configuration is $\theta_i = (79°, 20°, 171°)^T$, and the final arm configuration is $\theta_f = (115°, 81°, 75°)^T$. Figure 13 (configuration *c*) shows the final arm position when the shoulder angle is suddenly braked during the trajectory when it reaches 105° and is held fixed at this angle. The initial θ_i is the same as in the unperturbed case, and the pointer's distal end reaches precisely the same spatial x_1x_2 target as in the unperturbed motion, despite the fact that the final configuration has changed to $\theta_f = (105°, 95°, 52°)^T$. In other words, the system's response to

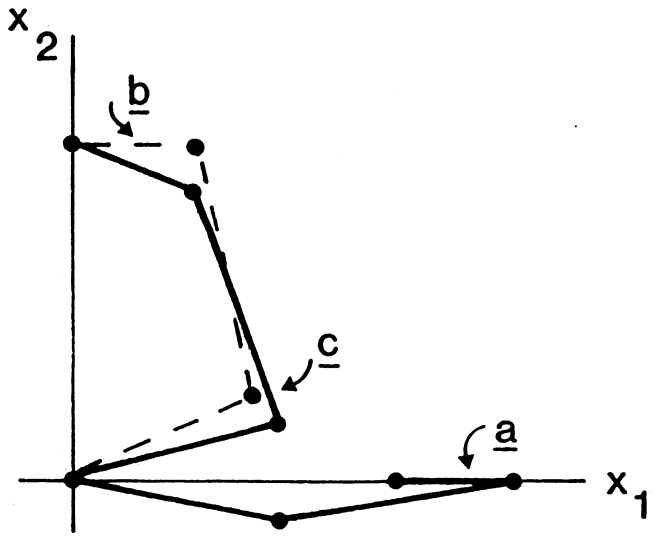

Figure 13. Arm configurations for simulated discrete reaches showing (a) initial posture, (b) final posture (unperturbed trajectory), and (c) final posture (perturbed trajectory).

the perturbation was to "automatically" redistribute the activity among its component degrees of freedom in a manner that still achieved the same task-space goal. Furthermore, such compensatory motor equivalence reflects the fact that targets in the task-dynamic model are not specified as final articulator configurations, but rather as desired spatial coordinates for the terminal device. The final articulator configuration "falls out" of the task-dynamic organization and the environmental conditions in which the movement is performed.

Relevance to Physiological Literature

In this section, we describe how task dynamics might apply to the issue of postural control in humans, and we suggest an alternative to the modular synergy model of Nashner and colleagues to account for postural compensatory phenomena (e.g., Nashner, 1981; Nashner & Woolacott, 1979; see also Saltzman & Kelso's [1985] commentary on Nashner & McCollum, 1985). Furthermore, we review evidence from single-joint discrete movement tasks (e.g., Bizzi, Chapple, & Hogan, 1982) showing that the physiologically relevant parameter of rest angle (i.e., the angle specified by the equilibrium point between agonist and antagonist length–tension curves) is actively specified during these tasks as a gradually (as opposed to steplike) changing central control signal. In the control law version of task dynamics, there is no articulator-dynamic control parameter corresponding to rest angle. However, a network coupling version of task dynamics, now in preliminary form, is described that includes rest angle as a parameter. Additionally, it provides a rational account for the evolution of the rest angle's trajectory without requiring an explicitly preplanned trajectory representation to account for the observed pattern.

Postural Control

Nashner and his colleagues have performed an elegant series of experiments on the postural responses of standing human subjects to perturbations of the support surface. Summarizing from the experimental report of Nashner, Woolacott, and Tuma (1979) and several subsequent reviews (Nashner, 1979; Nashner, 1981; Nashner & Woolacott, 1979), their paradigm and findings can be described in the following way. Basically, a subject stands with each foot on a separate horizontal platform that can be translated horizontally, translated vertically, or rotated about an axis aligned with the ankle joint. Using these platforms, one or a combination of the following four types of perturbation can be delivered to the subjects on a given trial (Figure 14): (a) simultaneous forward or backward anteroposterior translation (AP translation), (b) simultaneous flexion or extension rotation (direct rotation), (c) simultaneous upward or downward vertical translation (synchronous vertical), and (d) reciprocal vertical translation (reciprocal vertical). These perturbation types can be characterized by the corresponding patterns of whole body motions and joint rotations that would be induced in passive noncompensating subjects (Figure 14). Thus, AP translation causes the body to lean in the direction opposite to the translation, direct rotation causes the body to tilt in the same sense as the rotation, synchronous vertical causes the body to move with the translation, and reciprocal vertical causes the body to tilt laterally toward the lowering platform. The first three perturbation types induce motions in the sagittal plane, whereas the reciprocal vertical type induces motion in the frontal plane.

In response to each perturbation type or type combination, Nashner et al. measured electromyographic (EMG) responses from the upper and lower leg muscles, as well as changes in ankle, knee, and hip angles. Associated with each perturbation type was a long latency (e.g., 100–110 ms latency in gastrocnemius) "rapid postural adjustment" (Nashner, 1981), which constituted the earliest useful postural response, whereas the shorter latency myotatic reflexes were either absent or of no apparent functional value. These rapid postural adjustments for a given type were (a) characterized by fixed ratios of activity among the responding muscles, (b) specific to the perturbation type (and the corresponding type-specific patterns of joint displacements), and (c) "functionally related to the task of coordinating one kind of postural adjustment" (Nashner, 1979, p. 179). Furthermore, during a set of trials in which a sequence of either of three perturbation types (AP translation, synchronous vertical, or reciprocal vertical) was unexpectedly and immediately followed by a sequence of one of the other two types, the functionally appropriate postural synergy response occurred even on the first trial of the new type. Such first-trial adaptation did not occur, however, when a sequence of AP translations was followed immediately by an unexpected series of direct rotations (or vice versa). In these cases, the functionally correct (i.e., posturally stabilizing) synergistic response pattern was implemented progressively over a series of approximately three to five trials. Additionally (Horak & Nashner, 1983), if a series of AP trials with the subject standing directly on the footplates was followed by a series of AP trials with the feet resting on narrow transverse beams, the subject switched from a postural response involving predominantly ankle motions (ankle strategy) to one involving predominantly hip motions (hip strategy). This strategy change was implemented progressively over the course of approximately 5–20 trials, and this multitrial adaptation was

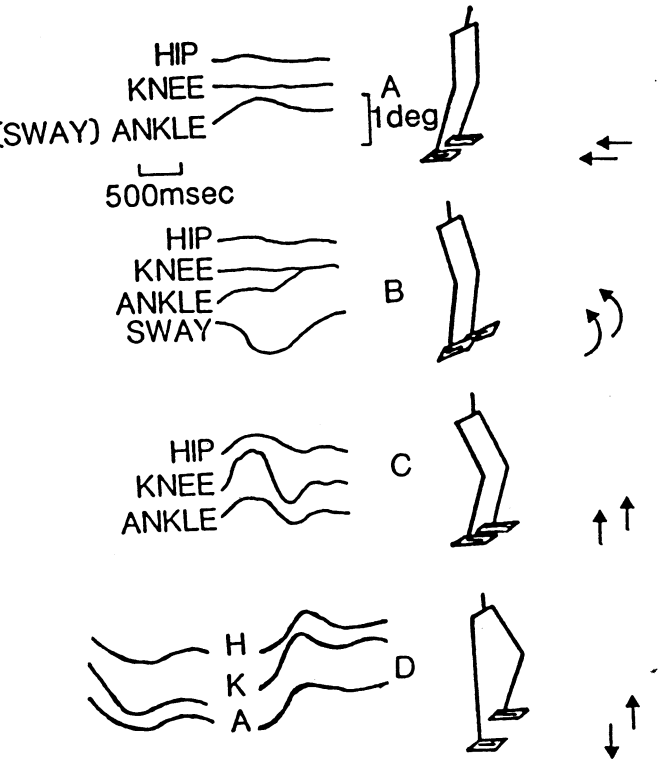

Figure 14. Description of basic postural perturbation paradigm of Nashner and colleagues, showing four types of perturbation (right column) and corresponding leg joint angular rotations (left column) (A: AP translation; B: direct rotation; C: synchronous vertical; D: reciprocal vertical). [From "The organization of rapid postural adjustments of standing humans: An experimental-conceptual model" by L. M. Nashner & M. Woolacott, 1979, In *Posture and movement* (p. 246) edited by R. E. Talbott & D. R. Humphrey, New York: Raven Press. Copyright 1979 by Raven Press. Adapted by permission.]

also seen for the reverse change from beam to footplate postural strategies.

Nashner and his colleagues have interpreted these data as being consistent with a modular synergy "conceptual model for the organization of postural adjustments" (e.g., Nashner, 1979, 1981; Nashner & Woolacott, 1979; see also Nashner & McCollum, 1985). Although it is admittedly in preliminary form, this hierarchical model proposes that postural synergies are organized spinally as separate modular function generators and are automatically triggered by correspondingly appropriate distinctive features of somatosensory (i.e., proprioceptive information related to joint angular rotations) inputs. Thus, for example, the AP sway synergy module is activated in proportion to ankle rotational input, whereas the vertical suspensory synergy module is activated in proportion to knee rotational input, and inhibition of the sway module by the suspensory module is provided to prevent simultaneous activation of both synergies. Such a system provides a reasonable account of the automatic first-trial postural responses described above. Additionally, supraspinal processes are assumed to modulate the input–output relationships of the peripheral synergy modules in order to maintain postural stability by using posturally relevant knowledge of results (e.g., sensory conflict between somatosensory and vestibular sources of information concerning the body's orientation relative to the support base and the line of gravity). Such supraspinal modulation is presumed to occur relatively slowly and is posited to underlie the multitrial adaptation phenomena described above.

Task-dynamics offers an attractive alternative to this hierarchical modular synergy approach. In the modular approach, synergies are canonically represented as stored output patterns and are triggered by corresponding distinctive features of somatosensory inputs. When the problem of postural control is formulated in task-dynamic terms, however, synergies need not be canonically represented anywhere; rather, synergistic patterns of muscle activity may be viewed as emergent properties of the task dynamically organized postural system (see also Saltzman & Kelso, 1985). In this latter view, one begins by defining a postural task space. For purposes of illustrative simplicity, postural control is described only in the sagittal plane, and the task space is modeled as a two-dimensional point attractor (see Figure 15A) for which (a) the terminal device is the body's center of mass and is represented as a point mass with mass m_T equal to total body mass (note that, unlike earlier examples, this terminal device cannot in general be associated with a particular point on the linkage system); (b) axis t_2 is defined parallel to the line of gravity and axis t_1 is defined normal to t_2; and (c) the t_1t_2 origin is defined by the target location of the mass center, which coincides with the mass center's initial location (assuming a posturally stable initial body configuration). The task-space equations of motions are

$$m_T\ddot{t}_1 + b_{T_1}\dot{t}_1 + k_{T_1}t_1 = 0; \tag{33}$$

$$m_T\ddot{t}_2 + b_{T_2}\dot{t}_2 + k_{T_2}t_2 = 0, \tag{34}$$

where damping and stiffness parameters define point-attractor topologies along each task axis. Gravity does not appear explicitly in Equation 34 inasmuch as t_2 denotes displacement from the statically stable vertical position of the task mass in the gravitational field. In other words, $t_2 = t_2^* - (m_T g/k_{T_2})$, where t_2^* corresponds to the statically stable vertical position of the task mass in the absence of gravity, and g denotes the acceleration due to gravity. In matrix form these equations become

$$M_T\ddot{\mathbf{t}} + B_T\dot{\mathbf{t}} + K_T\mathbf{t} = \mathbf{0}. \tag{35}$$

The task-space dynamical regime in Equation 35 can be transformed into body-space form with reference to a coordinate system whose origin coincides with the center of the support base. The spatial relationships between task space and body space are illustrated in Figure 15B, where (a) the x_1 axis is defined along the anteroposterior line between the rear and front edges (denoted by open squares) of the support base, which is defined by the contact areas between the feet and ground surface; (b) the x_2 axis is defined normal to x_1 at the midpoint of the support base; (c) the relative orientation between task and body space is defined by the angle Φ; and (d) the location of the task-space origin in body space coordinates is defined by $\mathbf{x}_0$. Both Φ and $\mathbf{x}_0$ are defined by the current postural configuration, which is assumed to be statistically stable; that is, the projection of the initial location of the center of mass (task-space origin) along the line of gravity falls within the boundaries of the support base. In this regard, the task-dy-

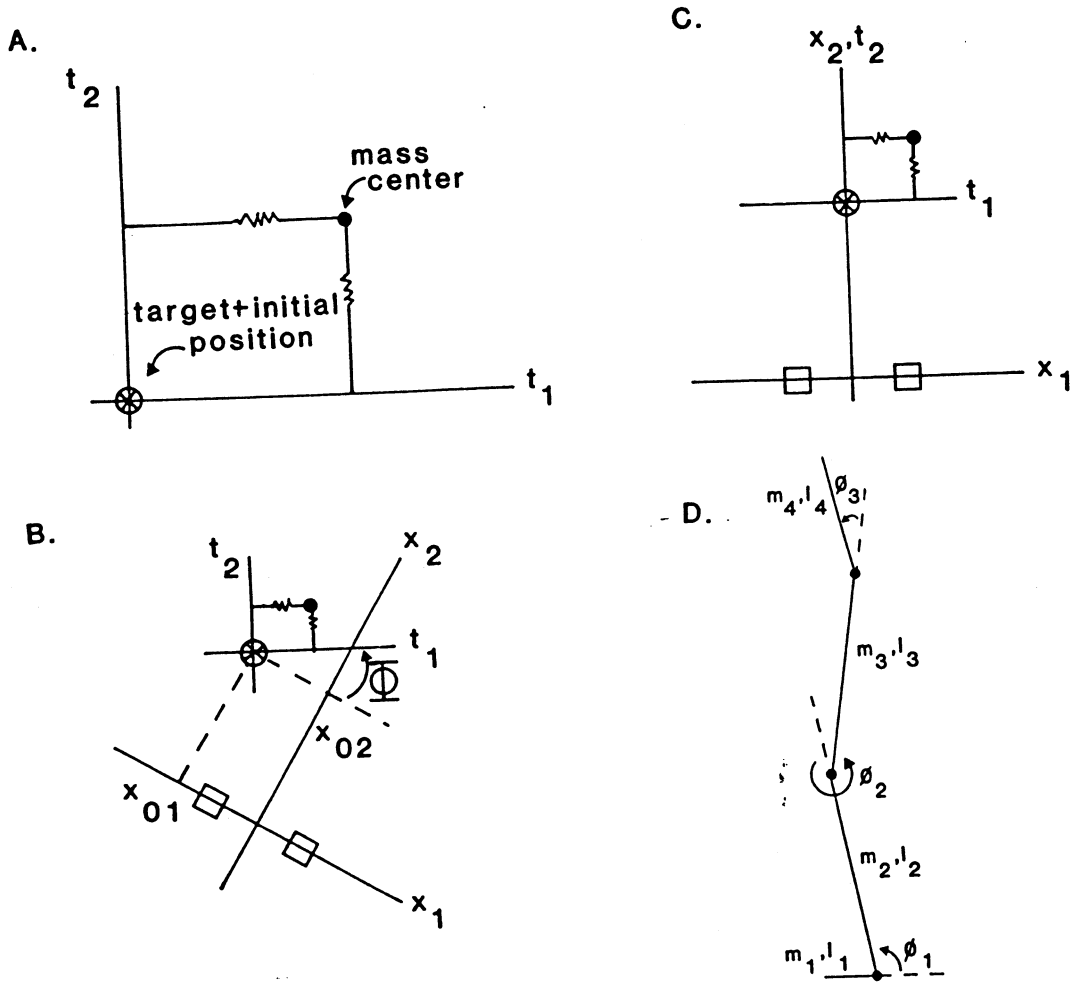

Figure 15. Postural maintenance task. (A: task space; B: body space. Open boxes represent front and back edges of support base [feet]; orientation angle, Φ, between task and body space is nonzero. C: body space. Φ is zero, representing parallel orientation of t_1 and x_1. D: postural effector system.)

namic model of vertical posture control is similar to the model proposed by Litvintsev (1972), who stated that it is likely that "the essential role in equilibrium maintenance is played by a mechanism which organizes muscular control at the various joints by parameters characterizing the general body position" (p. 590) and that "the magnitude and the rate of deviation of the weight center projection on the support plane are input parameters for this mechanism" (p. 598). Finally, note that (a) in most daily activities one stands on horizontal surfaces, and Φ thereby usually assumes a value of zero (Figure 15C), and (b) the body-space equations of motion derived from Equation 35 have the same form as Equation 6 in our earlier discrete reaching example.

The body-space dynamical regime can be transformed into an equivalent task-network expression based on the joint variables of a (simplified) model effector system (Figure 15D) with four segments (foot, shank, thigh, torso) and three joints (ankle, knee, hip). This task-network equation has the same general form as the discrete reaching equation (Equation 8), except that the task network for postural control involves three joints (not two joints) and two spatial variables. Consequently, the model effector system for postural adjustment tasks is redundant (see Footnote 7), and the mapping from body space to model effector coordinates requires the Jacobian pseudoinverse, J^+, or weighted pseudoinverse, J^*.

In task dynamics, consistent synergistic patterns of postural responses will occur in response to given types of destabilizing inputs. If a task network is established according to an accurate evaluation of the spatial relationships between task space and body space, these postural responses will be stabilizing and compensatory. Furthermore, they will be immediately accurate, in that they depend only upon the current limb state and the (accurately tuned) task network. In other words, synergistic responses emerge from the (tuned) postural system's underlying task-dynamic organization. There is no need to invoke the notion of access to and triggering of stored canonical synergy output programs. However, the postural system can be fooled into establishing an improperly tuned task network based either on an inappropriate evaluation of the geometric relationship between task space and body space or on the use of an inappropri-

ate weighting strategy for the joints in the (redundant) postural effector system. In the former case, for example, a series of trials involving AP translation perturbations requires tuning $\Phi = 0$, because the support base is horizontal throughout the trials. If a direct rotation perturbation is unexpecedly introduced, this setting is no longer valid and the task network will shape postural responses that are inappropriate and destabilizing for the new task-space–body-space geometry. Adaptive responses to direct rotation perturbations require setting $\Phi = \phi_1$ (where ϕ_1 = ankle angle) in order to tune the task network appropriately. Apparently, this sort of retuning process does not occur instantaneously but requires 3–5 trials, as discussed earlier.

In the case of tunings related to effector system weighting strategies, it appears that an efficient strategy for dealing with AP translations is an ankle-predominant one when the feet rest directly on the foot plates but a hip-predominant one when the feet rest on narrow beams. In the task-dynamic model, these strategies correspond to different tunings of the weighting matrices (associated with the weighted pseudoinverse, J^*) for the task network that depend on the current support surface. If the support surface condition is changed, say, from plate to beam support, then the ankle-weighted J^* used for the plate support will be inappropriate for (or less efficient than) the new beam support. Apparently, adaptively retuning J^* to reflect a hip-predominant strategy (and vice versa for hip to ankle strategy retuning) requires approximately 5–20 trials, as discussed earlier.

Rest Angle Trajectories and Network Coupling

Rest angles: Final position control, trajectory formation. It was noted earlier (in the topology and dynamics section) that discrete target-acquisition tasks in one-degree-of-freedom systems (e.g., at the elbow joint) displayed properties homologous to damped mass-spring systems (e.g., Cooke, 1980; Fel'dman, 1966; Kelso, 1977; Polit & Bizzi, 1978; Schmidt & McGown, 1980). These tasks had been modeled, essentially, as point attractors in an articulator-dynamic sense, requiring only the setting of the final or target rest-angle parameter (but see Footnote 4). According to the so-called "final position control" hypothesis (e.g., Bizzi, Accornero, Chapple, & Hogan, 1981; Kelso & Holt, 1980; Sakitt, 1980), the relative levels of neural activation of the springlike agonist and antagonist muscle groups at a joint

> define an equilibrium point between two opposing length–tension curves and consequently a joint angle. It has been suggested that the transition from a given position to another may occur whenever the CNS (central nervous system) generates a signal shifting the equilibrium point between the two muscles by selecting a new pair of length–tension curves. (Bizzi et al., 1981, p. 312)
>
> According to this schema, movements are, at the simplest level, transitions in posture. This simple idea is attractive because the details of the movement trajectory will be determined by the inertial and visco-elastic properties of muscles and ligaments around the joint. (Bizzi et al., 1981, p. 311–312)

However, as described above, such an articulator-dynamic scheme breaks down when more complex multijoint tasks are considered (see also Footnote 4). Furthermore, even for single-degree-of-freedom positioning tasks, the final position control hypothesis may be incomplete. Bizzi and his colleagues (Bizzi & Abend, 1982; Bizzi et al., 1981; Bizzi, Accornero, Chapple, & Hogan, 1982; Bizzi, Chapple, & Hogan, 1982), for example, have suggested that the rest angle trajectory itself is controlled in addition to final position. The final position control hypothesis predicts that elbow movements result from rapid shifts of the rest angle parameter to target equilibrium values and that, consequently, steady-state equilibrium positions would be achieved after a delay from muscle activity onset owing solely to the dynamics of muscle activation. Bizzi, Chapple, and Hogan (1982) offer a "slowest case" approximation of 150 ms for the time taken by the net muscle force to rise within a few percentage points of its final value. In fact, however, these investigators showed that for movements of at least 600 ms in duration, the mechanical expression of alpha motoneuronal activity reached steady state only after at least 400 ms had passed following the onset of muscle activity. Consequently, it appears that the centrally generated rest angle parameter gradually changes during the movement, even in deafferented monkeys, such that the alpha motoneuronal activity defines "a series of equilibrium positions, which constitute a trajectory whose end point is the desired final position" (Bizzi, Chapple, & Hogan, 1982, p. 398). Bizzi et al. (1981) interpreted their observations as implying the existence of trajectory plans or programs to account for the observed time courses of rest angle movement as well as the final rest angle position.

The control law version of task dynamics is unable to account for these data for two reasons. First, there is no parameter corresponding to rest angle in the single-degree-of-freedom case or rest configuration in the multi-degree-of-freedom case. Second, the control law version assumes that θ and $\dot{\theta}$ (real arm state) are perceived proprioceptively, that ϕ and $\dot{\phi}$ (model arm state) equal the real arm's state, and that control laws are specified according to the currently perceived real arm's state. In the "deafferented" case, in which the current θ and $\dot{\theta}$ are unavailable, the control laws are undefined and (coordinated) motion is not possible. Given the above "trajectory formation" data of Bizzi and colleagues, if task-dynamics is to be applied in these situations, the control law version must be amended to generate coordinated movements in deafferented preparations and to include a rest configuration parameter (which, of course, should evolve autonomously during the movement according to task-dynamic constraints). Although it is in preliminary form, we believe a network coupling version of task dynamics satisfies these requirements and provides a more biologically plausible task-dynamic account of skilled movements.

Network coupling. The network coupling method (outlined in Figure 16) involves shaping articulator dynamics according to task-specific dynamical constraints and may closely approximate a biological style of coordination and regulation. Briefly, network coupling involves interpreting the observed skilled motion of an effector system to be the observable output of an articulator network that makes up, however, only one half of a task-specific action system. The complete action system consists of the mutually or bidirectionally coupled task network (output variables: ϕ, $\dot{\phi}$, $\ddot{\phi}$, etc.) and articulator network (output variables: θ, $\dot{\theta}$, $\ddot{\theta}$, etc.). Thus, for the multi-degree-of-freedom discrete reaching task described earlier, this method involves (a) treating the task network defined by the model arm equation (Equation 8) as a system for intrinsic pattern generation that is specified for a given task and actor–environment context, and

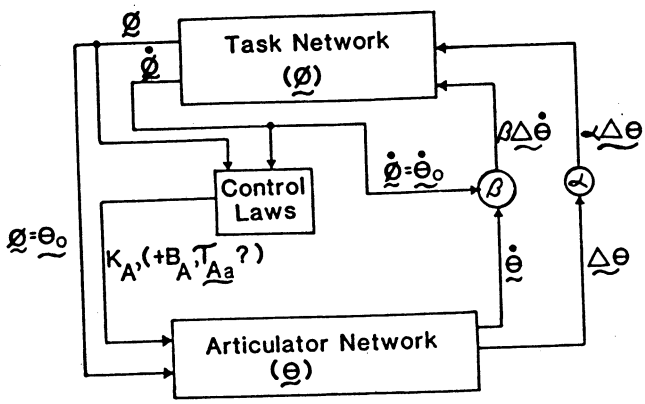

Figure 16. Overview of information flow in network coupling version of task dynamics.

that does not require peripheral input for its operation; (b) defining the articulator network corresponding to an actual arm by the following version of Equation 11:

$$\ddot{\theta} + M_A^{-1}S_A\dot{\theta}_p + M_A^{-1}B_A\dot{\theta} + M_A^{-1}K_A\Delta\theta + M_A^{-1}\tau_{Aa} = 0; \quad (36)$$

and (c) using the task network (i.e., the model arm's circuitry) to both actuate and modulate the real arm's behavior, while using the ongoing state of the real arm to modulate the task network.

The network coupling method begins by using the ongoing configuration of the model arm, ϕ, as the output of the task network. This output is delivered to the real arm as the ongoing "rest configuration" input, θ_0, for the articulator network (i.e., $\theta_0 = \phi$). However, because the task and articulator networks are potentially independent, one cannot simply assume identical states for the model arm and real arm (as in the control law approach). Rather, we make the less stringent assumption that real arm and model arm states are "close," that is, that $\theta - \phi = \Delta\theta$ and $\dot{\theta} - \dot{\phi} = \Delta\dot{\theta}$ are "small." Therefore, the constraint relationships for B_A, K_A, and τ_{Aa} are defined in a more approximate sense than those in Equations 13–15 (see Appendix for details):

$$B_A = [M_A J^{-1} M_B^{-1} B_B J]|_{\theta_0 = \phi}; \quad (37)$$

$$K_A = [M_A J^{-1} M_B^{-1} K_B J]|_{\theta_0 = \phi}; \quad (38)$$

$$\tau_{Aa} = \{[M_A J^{-1} V - S_A]|_{\theta_0 = \phi}\}\dot{\phi}_p. \quad (39)$$

These sets of driving constraints ($\theta_0 = \phi$) and modulating constraints (Equations 37–39) make up the efferent aspect of our coupled-network action system. With these constraints, the real arm becomes (statically) stable about the current rest configuration, with stiffness and damping properties defined relative to task-space axis directions.[10]

However, a coupled-network action system involves bidirectional coupling and, hence, an afferent aspect as well. This pattern of afference serves to modulate the activity of the task network on the basis of both relative angular displacement ($\Delta\phi = \phi - \theta$) and relative angular velocity ($\Delta\dot{\phi} = \dot{\phi} - \dot{\theta}$) coupling terms defined by $\alpha\Delta\phi$ and $\beta\Delta\dot{\phi}$, respectively, where α and β are constant scalar coupling coefficients. This type of coupling, which is proportional to differences between corresponding sets of state variables, is called *diffusive coupling* (e.g., Rand & Holmes, 1980). The modulated task network is then described by the following amended version of Equation 8:

$$\ddot{\phi} + J^{-1}M_B^{-1}B_B J\dot{\phi} + J^{-1}M_B^{-1}K_B\Delta x(\phi) + J^{-1}V\dot{\phi}_p + \alpha\Delta\phi + \beta\Delta\dot{\phi} = 0, \quad (40)$$

where, by assumption, $\Delta\phi$ and $\Delta\dot{\phi}$ are assumed small. The effects of these coupling terms on system behavior are to reduce the size of $\Delta\phi(= -\Delta\theta)$ via $\alpha\Delta\phi$ coupling and to reduce the size of $\Delta\dot{\phi}$ via $\beta\Delta\dot{\phi}$ coupling. In other words, these coupling terms act to maintain an in-phase (vs. anti-phase) one-to-one relationship between motions of the real and model arms. Equation 40 reverts to Equation 8 when $\Delta\phi$ and $\Delta\dot{\phi}$ equal zero (i.e., there is perfect mutual tracking of the real and model arms) or when the afferent coupling is disengaged (i.e., peripheral feedback is eliminated and the system is deafferented) by setting α and β to zero. Furthermore, even when deafferented the model arm is governed by the task-network equation (Equation 40), and hence, θ is capable of coordinated (although probably degraded) motion owing to internal feedback of the model arm's current state within the task network. Here, *internal feedback* is used in the sense of Evarts (1971) to indicate information "arising from structures within the nervous system" (p. 96) as opposed to peripheral information from proprioceptive sources in the (real) limbs. Finally, note that regulating $\Delta\phi(= -\Delta\theta)$ and $\Delta\dot{\phi}(= -\Delta\dot{\theta})$ to be small serves two purposes in the operation of the coupled action system: (a) It allows motion trajectories of the real arm to approximate those of the model arm, and (b) it serves to validate the small relative displacement and velocity assumptions used for the real arm control matrices specified in Equations 37–39.

The network coupling version of task dynamics provides a more biologically plausible sensorimotor control scheme than does the control law version. For single-degree-of-freedom positioning tasks, it provides a rational account of the centrally specified rest angle's trajectory for these tasks without invoking an explicitly preplanned representation of that trajectory. Rather, the rest angle trajectory evolves, even in the deafferented case, as an ongoing function of the tuned task network. Similarly, when applied to discrete planar reaching tasks of two-joint arms, the rest configuration trajectory will evolve so that the hand should move in a quasi-straight line from initial to final position. Finally, when applied to cyclic spatial movements of a multijoint arm, the network coupling approach shares certain features with recent views on the neural control of locomotion (see Grillner, 1981, for review). Investigators in this field assume the existence of innate, endogenous, cellular networks (i.e., so-called central pattern generators) that are (a) capable

[10] For task spaces not defined by linear dynamical regimes along each task axis, however, Equation 37 will no longer hold. For example, if a given task has a limit cycle organization for one task axis, and therefore a nonlinear damping term, the B_T and, hence, B_B matrices will reflect only the linear negative part of this damping. If B_B were used in Equation 37, the articulator network should be highly unstable. In such cases, however, one might simply choose B_A to make the articulator network stable about θ_0, given the K_A specified in Equation 38.

of driving the limbs according to the locomotor task without requiring peripheral information yet (b) can be modulated in phase-dependent ways by this same peripheral input (e.g., Forssberg, Grillner, & Rossignol, 1975). In this context, task networks can be interpreted as the abstract, learned analogs of such concretely defined, innate networks. Importantly, both task networks and central pattern generators instantiate specific task functions in their "circuitry" or architecture.

Presumably, however, task networks can be instantiated by a variety of physical, physiological, and neural mechanisms. Yet, to reemphasize, the main concern of task dynamics is to formalize in general and abstract terms a dynamical account of the functional cooperativities underlying the coordination and control of skilled movements. Its focus is not on the specific hardware structures and processes that support coordinated movements. In this, it follows the lead of earlier developments in relational biology (e.g., Rashevsky, 1961; Rosen, 1978) and provides, in the specific domain of skilled actions, "a mathematical framework in which function, organization and behavior could be directly characterized and studied, apart from any structural basis" (Rosen, 1978, p. xv).

References

Abbs, J. H., & Gracco, V. L. (1984). Control of complex motor gestures: Orofacial muscle responses to load perturbations of the lip during speech. *Journal of Neurophysiology, 51,* 705–723.

Abraham, R. H., & Shaw, C. D. (1982). *Dynamics—The geometry of behavior.* Santa Cruz, CA: Aerial Press.

Asada, H. (1982). A geometrical representation of manipulator dynamics and its application to arm design. In W. J. Book (Ed.), *Robotics research and advanced applications* (pp. 1–8). New York: American Society of Mechanical Engineers.

Benati, M., Gaglio, S., Morasso, P., Tagliasco, V., & Zaccaria, R. (1980). Anthropomorphic robotics. I. Representing mechanical complexity. *Biological Cybernetics, 38,* 125–140.

Bernstein, N. A. (1967). *The coordination and regulation of movements.* London: Pergamon Press.

Bizzi, E. (1980). Central and peripheral mechanisms in motor control. In G. E. Stelmach & J. Requin (Eds.), *Tutorials in motor behavior* (pp. 131–143). Amsterdam: North-Holland.

Bizzi, E., & Abend, W. (1982). Posture control and trajectory formation in single and multiple joint arm movements. In J. E. Desmedt (Ed.), *Brain and spinal mechanisms of movement control in man: New developments and clinical applications.* New York: Raven Press.

Bizzi, E., Accornero, N., Chapple, W., & Hogan, N. (1981). Processes underlying arm trajectory formation. In C. Ajmone-Marsan & O. Pompeiano (Eds.), *Brain mechanisms of perceptual awareness and purposeful behavior (IBRO Monograph Series,* pp. 311–318). New York: Raven Press.

Bizzi, E., Accornero, N., Chapple, W., & Hogan, N. (1982). Arm trajectory formation in monkeys. *Experimental Brain Research, 46,* 139–143.

Bizzi, E., Chapple, W., & Hogan, N. (1982). Mechanical properties of muscles: Implications for motor control. *Trends in Neurosciences, 5,* 395–398.

Cooke, J. D. (1980). The organization of simple, skilled movements. In G. E. Stelmach & J. Requin (Eds.), *Tutorials in motor behavior* (pp. 199–212). Amsterdam: North-Holland.

Delatizky, J. (1982). *Final position control in simulated planar horizontal arm movements.* Unpublished doctoral dissertation, Massachusetts Institute of Technology, Department of Electrical Engineering and Computer Science.

Dorf, R. C. (1974). *Modern control systems* (2nd ed.). Reading, MA: Addison-Wesley.

Evarts, E. V. (1971). Feedback and corollary discharge: A merging of the concepts. *Neurosciences Research Program Bulletin, 9,* 86–112.

Fel'dman, A. G. (1966). Functional tuning of the nervous system with control of movement or maintenance of a steady posture. III. Mechanographic analysis of execution by man of the simplest motor tasks. *Biophysics, 11,* 766–775.

Fel'dman, A. G., & Latash, M. L. (1982). Interaction of afferent and efferent signals underlying joint position sense: Empirical and theoretical approaches. *Journal of Motor Behavior, 14,* 174–193.

Folkins, J. W., & Abbs, J. H. (1975). Lip and jaw motor control during speech: Responses to resistive loading of the jaw. *Journal of Speech and Hearing Research, 18,* 207–220.

Forssberg, H., Grillner, S., & Rossignol, S. (1975). Phase dependent reflex reversal during walking in chronic spinal cats. *Brain Research, 55,* 247–304.

Fowler, C. (1977). *Timing control in speech production.* Bloomington, IN: Indiana University Linguistics Club.

Fowler, C. A., Rubin, P., Remez, R. E., & Turvey, M. T. (1980). Implications for speech production of a general theory of action. In B. Butterworth (Ed.), *Language production.* New York: Academic Press.

Georgopoulos, A. P., Kalaska, J. F., & Massey, J. T. (1981). Spatial trajectories and reaction times of aimed movements: Effects of practice, uncertainty, and change in target location. *Journal of Neurophysiology, 46,* 725–743.

Greene, P. H. (1971). Introduction. In I. M. Gelfand, V. S. Gurfinkel, S. V. Fomin, & M. L. Tsetlin (Eds.), *Models of the structural-functional organization of certain biological systems.* Cambridge, MA: MIT Press.

Grillner, S. (1981). Control of locomotion in bipeds, tetrapods, and fish. In J. M. Brookhart & V. B. Mountcastle (Eds.), *Handbook of physiology, Section 1: The nervous system, Vol. II: Motor control, Part 1* (pp. 1179–1236). Bethesda, MD: American Physiological Society.

Grillner, S. (1982). Possible analogies in the control of innate motor acts and the production of sound in speech. In S. Grillner, B. Lindblom, J. Lubker, & A. Persson (Eds.), *Speech motor control* (pp. 217–229). Oxford: Pergamon Press.

Hebb, D. O. (1949). *The organization of behavior.* New York: Wiley.

Hogan, N. (1980). Mechanical impedance control in assistive devices and manipulators. In B. Friedland & H. A. Spang (Eds.), *Proceedings of the 1980 joint automatic control conference, Vol. 1* (Paper TA 10-B). San Francisco: American Automatic Control Council.

Hogan, N., & Cotter, S. L. (1982). Cartesian impedance control of a nonlinear manipulator. In W. J. Book (Ed.), *Robotics research and advanced applications* (pp. 121–128). New York: American Society of Mechanical Engineers.

Hollerbach, J. M. (1982). Computers, brains, and the control of movement. *Trends in Neurosciences, 5,* 189–192.

Hollerbach, J. M., & Flash, T. (1981). *Dynamic interactions between limb segments during planar arm movement* (AIM-635). Boston: Massachusetts Institute of Technology, Artificial Intelligence Laboratory.

Horak, F., & Nashner, L. (1983). Two distinct strategies for stance posture control: Adaptation to altered support surface configuration. *Society of Neuroscience Abstracts, 10,* 65.

Ito, M. (1982). Questions in modeling the cerebellum. *Journal of Theoretical Biology, 99,* 81–86.

Jordan, D. W., & Smith, P. (1977). *Nonlinear ordinary differential equations.* Oxford, England: Clarendon Press.

Kelso, J. A. S. (1977). Motor control mechanisms underlying human movement reproduction. *Journal of Experimental Psychology: Human Perception and Performance, 3,* 529–543.

Kelso, J. A. S. (1981). Contrasting perspectives on order and regulation in movement. In J. Long & A. Baddeley (Eds.), *Attention and performance* (Vol. 9). Hillsdale, NJ: Erlbaum.

Kelso, J. A. S., & Holt, K. G. (1980). Exploring a vibratory systems analysis of human movement production. *Journal of Neurophysiology, 43,* 1183–1196.

Kelso, J. A. S., Holt, K. G., Kugler, P. N., & Turvey, M. T. (1980). On the concept of coordinative structures as dissipative structures: II. Empirical lines of convergence. In G. E. Stelmach & J. Requin (Eds.), *Tutorials in motor behavior* (pp. 49–70). New York: North-Holland.

Kelso, J. A. S., Holt, K. G., Rubin, P., & Kugler, P. N. (1981). Patterns of human interlimb coordination emerge from the properties of nonlinear limit cycle oscillatory processes: Theory and data. *Journal of Motor Behavior, 13,* 226–261.

Kelso, J. A. S., & Saltzman, E. L. (1982). Motor control: Which themes do we orchestrate? *Behavioral and Brain Sciences, 5,* 554–557.

Kelso, J. A. S., Saltzman, E. L., & Tuller, B. (1986a). The dynamical perspective in speech production: Data and theory. *Journal of Phonetics, 14,* 29–59.

Kelso, J. A. S., Saltzman, E. L., & Tuller, B. (1986b). Intentional contents, communicative context, and task dynamics: A reply to the commentators. *Journal of Phonetics, 14,* 171–196.

Kelso, J. A. S., Southard, D. L., & Goodman, D. (1979). On the coordination of two-handed movements. *Journal of Experimental Psychology: Human Perception and Performance, 5,* 229–238.

Kelso, J. A. S., Tuller, B., & Fowler, C. A. (1982). The functional specificity of articulatory control and coordination. *Journal of the Acoustical Society of America, 72,* S103.

Kelso, J. A. S., Tuller, B., & Harris, K. S. (1983). A 'dynamic pattern' perspective on the control and coordination of movement. In P. MacNeilage (Ed.), *The production of speech* (pp. 137–173). New York: Springer-Verlag.

Kelso, J. A. S., Tuller, B., Vatikiotis-Bateson, E., & Fowler, C. A. (1984). Functionally specific articulatory cooperation following jaw perturbations during speech: Evidence for coordinative structures. *Journal of Experimental Psychology: Human Perception and Performance, 10,* 812–832.

Khatib, O. (1985). The potential field approach and operational space formulation in robot control. In *Proceedings of the 4th Yale workshop on applications of adaptive systems theory, May 29–31, 1985* (pp. 208–214). New Haven, CT: Yale University Center for Systems Science.

Klein, C. A., & Huang, C.-H. (1983). Review of pseudoinverse control for use with kinematically redundant manipulators. *IEEE Transactions on Systems, Man, and Cybernetics, SMC-13,* 245–250.

Koditschek, D. E. (1985). Selection of natural motion via feedback. In *Proceedings of the 4th Yale workshop on applications of adaptive systems theory: May 29–31, 1985* (pp. 221–227). New Haven, CT: Yale University Center for Systems Science.

Kugler, P. N., Kelso, J. A. S., & Turvey, M. T. (1980). On the concept of coordinative structures as dissipative structures: I. Theoretical lines of convergence. In G. E. Stelmach & J. Requin (Eds.), *Tutorials in motor behavior* (pp. 3–47). New York: North-Holland.

Lashley, K. S. (1930). Basic neural mechanisms in behavior. *Psychological Review, 37,* 1–24.

Litvintsev, A. I. (1972). Vertical posture control mechanisms in man. *Automation and Remote Control, 33,* 590–600.

Mason, M. T. (1981). Compliance and force control for computer controlled manipulators. *IEEE Transactions on Systems, Man, and Cybernetics, SMC-11,* 418–432.

McGhee, R. B., & Iswandhi, G. I. (1979). Adaptive locomotion of a multi-legged robot over rough terrain. *IEEE Transactions on Systems, Man, and Cybernetics, SMC-9,* 176–182.

Minorsky, N. (1962). *Nonlinear oscillations.* Princeton, NJ: Van Nostrand.

Morasso, P. (1981). Spatial control of arm movements. *Experimental Brain Research, 42,* 223–227.

Munhall, K. G., & Kelso, J. A. S. (1985). Phase-dependent sensitivity to perturbation reveals the nature of speech coordinative structures. *Journal of the Acoustical Society of America, 78*(Suppl. 1), S38.

Nashner, L. M. (1979). Organization and programming of motor activity during posture control. In R. Granit & O. Pompeiano (Eds.), *Reflex control of posture and movement* (*Progress in Brain Research, Vol. 50,* pp. 177–184). New York: Elsevier/North-Holland Biomedical Press.

Nashner, L. M. (1981). Analysis of stance posture in humans. In A. L. Towe & E. S. Luschei (Eds.), *Handbook of behavioral neurobiology: Vol. 5: Motor cordination* (pp. 527–565). New York: Plenum.

Nashner, L. M., & McCollum, G. (1985). The organization of human postural movements: A formal basis and experimental synthesis. *Behavioral and Brain Sciences, 8,* 135–172.

Nashner, L. M., & Woolacott, M. (1979). The organization of rapid postural adjustments of standing humans: An experimental-conceptual model. In R. E. Talbott & D. R. Humphrey (Eds.), *Posture and movement* (pp. 243–257). New York: Raven Press.

Nashner, L. M., Woolacott, M., & Tuma, G. (1979). Organization of rapid responses to postural and locomotor-like perturbations of standing man. *Experimental Brain Research, 36,* 463–476.

Pellionisz, A., & Llinas, R. (1979). Brain modeling by tensor network theory and computer simulation. The cerebellum: Distributed processor for predictive coordination. *Neuroscience, 4,* 323–348.

Polit, A., & Bizzi, E. (1978). Processes controlling arm movements in monkeys. *Science, 201,* 1235–1237.

Raibert, M. H. (1978). A model for sensorimotor control and learning. *Biological Cybernetics, 29,* 29–36.

Raibert, M. H., Brown, H. B., Jr., Chepponis, M., Hastings, E., Shreve, S. E., & Wimberly, F. C. (1981). *Dynamically stable legged locomotion* (Technical Report CMU-RI-TR-81-9). Pittsburgh, PA: Carnegie Mellon University, Robotics Institute.

Raibert, M. T., & Craig, J. J. (1981). Hybrid position/force control of manipulators. *ASME Journal of Dynamic Systems, Measurement, and Control, 102,* 126–133.

Rand, R. H., & Holmes, P. J. (1980). Bifurcation of periodic motions in two weakly coupled van der Pol oscillators. *International Journal of Non-Linear Mechanics, 15,* 387–399.

Rashevsky, N. (1961). *Mathematical principles in biology and their applications.* Springfield, IL: Charles C Thomas.

Rosen, R. (1978). *Fundamentals of measurement and representation of natural systems.* New York: North-Holland.

Sakitt, B. (1980). A spring model and equivalent neural network for arm posture control. *Biological Cybernetics, 37,* 227–234.

Saltzman, E. L. (1979). Levels of sensorimotor representation. *Journal of Mathematical Psychology, 20,* 91–163.

Saltzman, E. L. (1986). Task dynamic coordination of the speech articulators: A preliminary model. In H. Heuer & C. Fromm (Eds.), *Generation and modulation of action patterns* (Experimental Brain Research Series 15, pp. 129–144). New York: Springer-Verlag.

Saltzman, E. L., & Kelso, J. A. S. (1985). Synergies: Stabilities, instabilities, and modes. *Behavioral and Brain Sciences, 8,* 161–163.

Schmidt, R. A. (1982). *Motor control and learning: A behavioral emphasis.* Champaign, IL: Human Kinetics.

Schmidt, R. A., & McGown, C. (1980). Terminal accuracy of unexpectedly loaded rapid movements: Evidence for a mass-spring mechanism in programming. *Journal of Motor Behavior, 12,* 149–161.

Soechting, J. F. (1982). Does position sense at the elbow joint reflect a sense of elbow joint angle or one of limb orientation? *Brain Research, 248,* 392–395.

Soechting, J. F., & Lacquaniti, F. (1981). Invariant characteristics of a pointing movement in man. *Journal of Neuroscience, 1,* 710–720.

Stein, R. B. (1982). What muscle variables does the central nervous system control? *Behavioral and Brain Sciences, 5,* 535–577.

Szentagothai, J., & Arbib, M. A. (Eds.). (1974). Conceptual models of neural organization. *Neurosciences Research Program Bulletin, 12*(3).

Takegaki, M., & Arimoto, S. (1981). A new feedback method for dynamic control of manipulators. *Journal of Dynamic Systems, Measurement, and Control, 102,* 119–125.

Turvey, M. T., Shaw, R. E., & Mace, W. (1978). Issues in the theory of action: Degrees of freedom, coordinative structures and coalitions. In J. Requin (Ed.), *Attention and performance VII* (pp. 557–595). Hillsdale, NJ: Erlbaum.

Viviani, P., & Terzuolo, V. (1980). Space-time invariance in learned motor skills. In G. E. Stelmach & J. Requin (Eds.), *Tutorials in motor behavior.* Amsterdam: North-Holland.

Whiting, H. T. A. (Ed.). (1984). *Human motor actions: Bernstein reassessed.* Amsterdam: North-Holland.

Whitney, D. E. (1972). The mathematics of coordinated control of prosthetic arms and manipulators. *ASME Journal of Dynamic Systems, Measurement and Control, 94,* 303–309.

Appendix

Equation 7

The body-spatial variables $(\mathbf{x}, \dot{\mathbf{x}}, \ddot{\mathbf{x}})$ of Equation 6 are transformed into the joint variables $(\phi, \dot{\phi}, \ddot{\phi})$ of a massless arm model using the following kinematic relationships:

$$\mathbf{x} = \mathbf{x}(\phi) \tag{A1}$$

$$\dot{\mathbf{x}} = J(\phi)\dot{\phi} \tag{A2}$$

$$\ddot{\mathbf{x}} = J(\phi)\ddot{\phi} + (dJ(\phi)/dt)\dot{\phi} = J(\phi)\ddot{\phi} + V(\phi)\dot{\phi}_p, \tag{A3}$$

where $\mathbf{x}(\phi)$ = the current body-spatial position vector of the terminal device expressed as a function of the current model arm configuration;
$= [(l_1\sin\phi_1 + l_2\sin(\phi_1 + \phi_2)), (-l_1\cos\phi_1 - l_2\cos(\phi_1 + \phi_2))]^T$;
$\dot{\phi}_p = [\dot{\phi}_1^2, \dot{\phi}_1\dot{\phi}_2, \dot{\phi}_2^2]^T$, the current joint velocity product vector;
$J(\phi)$ = the Jacobian transform matrix;

$$= \begin{bmatrix} (l_1\cos\phi_1 + l_2\cos(\phi_1 + \phi_2)) & l_2\cos(\phi_1 + \phi_2) \\ (l_1\sin\phi_1 + l_2\sin(\phi_1 + \phi_2)) & l_2\sin(\phi_1 + \phi_2) \end{bmatrix};$$

$V(\phi)$ = a 2×3 matrix resulting from rearranging the terms of the expression $(dJ(\phi)/dt)\dot{\phi}$ in order to segregate the joint velocity products into a single vector $\dot{\phi}_p$;

$$= \begin{bmatrix} (-l_1\sin\phi_1 - l_2\sin(\phi_1 + \phi_2)) & (-2l_2\sin(\phi_1 + \phi_2)) & (-l_2\sin(\phi_1 + \phi_2)) \\ (l_1\cos\phi_1 + l_2\cos(\phi_1 + \phi_2)) & (2l_2\cos(\phi_1 + \phi_2)) & (l_2\cos(\phi_1 + \phi_2)) \end{bmatrix}.$$

Making these substitutions into Equation 6 (text) and rearranging, we get Equation 7 (text):

$$M_B J\ddot{\phi} + B_B J\dot{\phi} + K_B\Delta\mathbf{x}(\phi) = -M_B V\dot{\phi}_p, \tag{A4), (7}$$

Note that because $\Delta\mathbf{x}$ in Equation 6 is not assumed small, the differential approximation $\mathbf{dx} = J(\phi)\mathbf{d}\phi$ is not justified. Therefore, Equation A1 was used instead for the kinematic displacement transformation into model arm variables.

Equation 9

Using a Lagrangian analysis (see, for example, Saltzman, 1979, for details), one may derive the passive mechanical equations of motion for the two-segment arm (frictionless, no gravity) described in the text:

$$M_A\ddot{\theta} + S_A\dot{\theta}_p = \mathbf{0}, \tag{B1), (9}$$

where $M_A = M_A(\theta)$, the 2×2 acceleration sensitivity matrix with elements q_{ij},

where $q_{11} = m_2(l_1^2 + (1/3)l_2^2 + l_1l_2\cos\theta_2) + m_1(1/3)l_1^2$;
$q_{12} = m_2((1/3)l_2^2 + (1/2)l_1l_2\cos\theta_2)$;
$q_{21} = q_{12}$;
$q_{22} = (1/3)m_2l_2^2$;

and where $S_A = S_A(\theta)$, a 2×3 matrix with elements s_{ij} resulting from rearranging the terms of the coriolis and centripetal torque terms in order to segregate the joint velocity products into a single vector $\dot{\theta}_p$,

where $s_{11} = 0$; $s_{12} = -m_2l_1l_2\sin\theta_2$; $s_{13} = (1/2)s_{12}$;
$s_{21} = -s_{13}$; $s_{22} = 0$; $s_{23} = 0$.

Equations 37–39

1. For K_A, we begin with the expression $M_A^{-1}K_A\Delta\theta|_{\theta_0-\phi}$ from Equation 36. Because we assume that $\Delta\theta$ is small, we are justified in making the differential approximation:

$$[M_A^{-1}K_A\mathbf{d}\theta]|_{\theta_0} = [M_A^{-1}K_AJ^{-1}\mathbf{dx}]|_{\theta_0}, \tag{C1}$$

where $\mathbf{dx} = \mathbf{x}(\theta) - \mathbf{x}(\theta_0)$ denotes the differential body-space displacement between the terminal devices of the real (articulator network) and model (task network) arms, and $[M_A^{-1}K_AJ^{-1}]|_{\theta_0}$ denotes the articulator stiffness pattern governing the real arm's responses to small displacements about $\mathbf{x}(\theta_0 = \phi)$.

The body-spatial stiffness responses of the model arm specified by task dynamics for (possibly) large scale displacements $\Delta\mathbf{x}(\phi) = \mathbf{x}(\phi) - \mathbf{x}_0$ from the reaching target $\mathbf{x}_0$ are governed by the spatial restoring force term $[J^{-1}M_B^{-1}K_B\Delta\mathbf{x}(\phi)]|_\phi$ in Equation 8. Assuming that the model ($\phi = \theta_0$) and real (θ) arm configurations are close, we compare the stiffness expressions and define the following constraint relationship:

$$K_A = [M_AJ^{-1}M_B^{-1}K_BJ]|_{\theta_0-\phi} \tag{C2}$$

This relationship specifies that stiffness responses of the real arm to small $\Delta\theta$ perturbations will be defined according to task-space axis directions and task-space stiffness weightings.

2. For B_A, τ_{As}, assuming that both $\Delta\theta$ and $\Delta\dot{\theta}$ are small, one may use equations 8, 13, and 15 to define the following constraint relationships:

$$B_A = [M_AJ^{-1}M_B^{-1}B_BJ]|_{\theta_0-\phi}, \tag{C3}$$

$$\tau_{As} = \{[M_AJ^{-1}V - S_A]|_{\theta_0-\phi}\}\dot{\phi}_p. \tag{C4}$$

Received June 20, 1984
Revision received January 15, 1986 ■